Molecular Breeding

On the genetic architecture in a public tropical maize panel of the symbiosis between corn and plant growth-promoting bacteria aiming to improve plant resilience

--Manuscript Draft--

Manuscript Number:	MOLB-D-21-00013R1
Full Title:	On the genetic architecture in a public tropical maize panel of the symbiosis between corn and plant growth-promoting bacteria aiming to improve plant resilience
Article Type:	Original Article
Keywords:	Shovelomics; root architecture; GWAS; symbiosis interaction; genomic prediction
Corresponding Author:	Rafael Massahiro Yassue Universidade de São Paulo Escola Superior de Agricultura Luiz de Queiroz: Universidade de Sao Paulo Escola Superior de Agricultura Luiz de Queiroz Piracicaba, SP BRAZIL
Corresponding Author Secondary Information:	
Corresponding Author's Institution:	Universidade de São Paulo Escola Superior de Agricultura Luiz de Queiroz: Universidade de Sao Paulo Escola Superior de Agricultura Luiz de Queiroz
Corresponding Author's Secondary Institution:	
First Author:	Rafael Massahiro Yassue
First Author Secondary Information:	
Order of Authors:	Rafael Massahiro Yassue
	Humberto Fanelli Carvalho
	Raysa Gevartosky
	Felipe Sabadin
	Pedro Henrique Souza
	Maria Leticia Bonatelli
	João Lúcio Azevedo
	Maria Carolina Quecine
	Roberto Fritsche-Neto
Order of Authors Secondary Information:	
Funding Information:	Fundação de Amparo à Pesquisa do Estado de São Paulo (17/24327-0) — Dr Roberto Fritsche-Neto
	Fundação de Amparo à Pesquisa do Estado de São Paulo (19/04697-2) — Dr João Lúcio Azevedo
	Coordenação de Aperfeiçoamento de Pessoal de Nível Superior (CAPES) (001) — Not applicable
	Conselho Nacional de Desenvolvimento Científico e Tecnológico (CNPq) — Not applicable
Abstract:	Exploring the symbiosis between plants and plant-growth-promoting bacteria (PGPB) is a new challenge for sustainable agriculture. Even though many works have reported the beneficial effects of PGPB in increasing plant resilience for several stresses, its potential is not yet widely explored. One of the many reasons is the differential symbiosis performance depending on the host genotype. This opens doors to plant breeding programs to explore the genetic variability and develop new cultivars with higher response to PGPB interaction and, therefore, have higher resilience to stress.

	Hence, we aimed to study the genetic architecture of the symbiosis between PGPB and tropical maize germplasm, using a public association panel and its impact on plant resilience. Our findings reveal that the synthetic PGPB population can modulate and impact root architecture traits, improve resilience to nitrogen stress, and 37 regions were significant for controlling the symbiosis between PGPB and tropical maize. We found two overlapping SNPs in the GWAS analysis indicating strong candidates for further investigations. Furthermore, genomic prediction analysis with genomic relationship matrix computed using only significant SNPs obtained from GWAS analysis substantially increased the predictive ability for several traits endorsing the importance of these genomic regions for the response of PGPB. Finally, the public tropical panel reveals a significant genetic variability to the symbiosis with the PGPB and can be a source of alleles to improve plant resilience.
Response to Reviewers:	Reviewer #1: The authors would like to thank Reviewer #1 for his suggestions, and we made substantial changes to the manuscript. We very much appreciate the contribution regarding the statistical test of significance, GWAS for the response, and the suggestion of adding the genomic prediction models to test the allelic combinations obtained from GWAS analysis and their predictive ability. Furthermore, a detailed point-by-point response to all the comments. Reviewer #1: Yassue, Carvalho, Gevartosky et al. present their analyses on the end of season response of maize underground tissues to the presence of plant growth promoting bacteria (PGPB). Following GWAS analyses, several candidate genes are identified. This topic is interesting and, since the interactions between plants and micro-organism are difficult to quantify, I fully understand how challenging such studies can be. The phenotypic data the authors collected can be a valuable data set for other researchers. Unfortunately, the analyses have been conducted improperly that make the results and conclusion very questionable. Major concerns: 1. I checked the Github page that authors provide for the trait extraction pipeline and found they are custom-built. Therefore, it is necessary conduct evaluations on the measurement consistency and the testing of accuracy on the pipeline the authors developed for the root phenotyping are missing in this paper. At least a comparison between auto-extracted root trait values and manual measurements, such as traits measured from same images using imageJ, shall be conducted. In order to evaluate the accuracy of the root-trait extraction pipeline from the author's pipeline, we validate the trait Convex Hull Area (CHA) using the software RhizoVision Explorer. The author's pipeline and the RhizoVision Explorer correlated 0.93 using 576 observations. For root angle (RA), we evaluate using the software ImageJ with 30 observations, and the correlation was 0.97. We used a lower number of observations for RA because the pipeline in the ImageJ is manual. We add this information in the Supplemental Figure 2. 2. There are no tests of statistic in the paper for the trait analyses. It is therefore unclear to what extent that root traits are different under B+ and B- environments. For some traits, such as RA, PH, it looks less likely there will be a significant difference on the population mean at all. Some traits there are clear differences on the magnitude of phenotypic variance between B+ and B- and shall be investigated too. We performed the statistical tests using LRT and Wald for random and fixed effects, respectively, and added this information in the text (Supplementary table 2.). 3. Since this study aiming the phenotypic variation of root architectures under the presence of PGPB. It is then natural to investigate the response of root traits with the presence of PGPB. It is clearly in the correlation figure listed as supplementary material that some traits the slopes are different between B+ and B- conditions. It will be very interesting analyses to conduct GWAS on the responses as well. In fact, the analyses on the response probably shall be the most important analyses in this paper yet get completely ignored by the authors. We agree with the reviewer's comments, and we performed the GWAS, heritability, and genomic prediction models for the response. 4. The authors use covariate matrix calculated from additive matrix. This is more computationally tractable approach because the dimensionality of the dataset can be

thus greatly reduced. But then you are also calculating a summary (PCA) of a summary (covariance matrix), so there's a sort of double reduction in the data. The FarmCPU.P.Threshold function was designed to control inflation yet from figure 2 (BTW this figure needs be seriously revised, pls checked minor comments) for some traits the results are still severely inflated. The GWAS can also be further optimized using the bin.selection function based on the estimated LD decay. You would find the bin.size is very large by default if you check the manual of FarmCPU.
We agreed with the reviewer's suggestions, although the correlation between the PCA analysis using the matrix of markers and the additive matrix is either -1 or 1 for the first ten principal components. Therefore, we believe that this should not impact the results. Regarding the bin.selection function, the authors did not feel comfortable altering the bin size, so we decided to follow the recommendation in the FarmCPU manual in using the default parameters.

5. The GWAS results in the manuscript are also interpreted improperly. Although the GWAS looks different between B+ and B-, it does not necessarily mean the causal effects on the responses of PGPB are different. It has been reported the phenotypic variations of underground traits are powered up by genes with small effect sizes. This makes it challenging for properly estimated the allelic effects using a relatively small population and thus even small amount of measurement errors can cause huge difference between two replicates. It is quite possible that the signals that B+ and B- GWAS identified are functional in both conditions. In addition, considering the size of LD decay provided by the authors, I'm less inclined to call any overlaps signals identified by their GWAS as "pleiotropic" as well.
We agree with the reviewer's comments, and we altered the term "pleiotropic" to "overlapping" SNPs or genes. Also, we add a brief explanation about it (L. 451-459).
From the supplementary figure, the estimated LD decay is actually very large on a genome-wide level. If set background r-squared as 0.1 you are probably going to get estimated LD decay close to 1Mb. Even using the same LD decay (200~300 kb), which means a close to 500kb intervals, the number of genes can be found in a genome region with such size will be high. Therefore, any following up analysis shall be conducted very carefully. Yet, I find no statistical testing been documented which makes all the following network analyses conducted by the authors been questionable. At least a test for randomness shall be conducted before calling any genes as "candidate". In fact, from a practical perspective, I would challenge the value of conducting such candidate gene and netwoks analyses to be necessary at all. It would be much more interesting to test how well different allelic combinations of those significant GWAS signals can be used to distinguish different root architecture or their predictability to root architecture. It would also be important to test whether that maize, both underground and above ground parts, can benefit from the PGPB in this population yet such data is not presented at all.
We agree with the reviewer's suggestions, and we made substantial changes in the analysis and interpretation. We remove the subnetworks analysis, and we add the genomic prediction analysis using the SNPs obtained from the GWAS analysis. Our results may endorse the importance of these genomic regions for the response of PGPB.
We also add the genotype by treatment analysis to obtain which traits are more related to which treatment.
At last, I would strongly recommend the authors to seriously revise their figures and tables especially the legend text (check the minor comments).

Minor comments:

-How the analysis of Figure 1 b was conducted is not documented in the M&M. It also shall be described in the legend of Figure 1 to distinguish with the kinship variance calculated by PCA using genotypic information, otherwise readers will be confused.
We add the principal components using the phenotypic traits in the supplementary, and we revise the legend.

-P-values in Table 2 are incorrectly presented, I guess those are -log10?
We correct this information in the text.

-Figure 2: GWAS traits are not distinguishable which basically makes this figure unreadable. Font size of Y-axis in 2a is too small.

We remake all the figures and add in supplementary figure 9-11.

-Figure 3 a: the number of genes overlapped between B+ and B- shall be labeled
We remake all the figures and correct them in the text.

-Supplementary materials are not properly appended. Legends are not clearly written as well, i.e. information of the abbreviations in supplemental is missing. This shall also be added to figure 1 and 3 in the main text as well.
We revise the figure and legends.

-The supplemental figure labeled as "Population analysis of public tropical maize panel" makes no sense at all. What is the Y-axis?
We add this information in the legends.

-Supplemental traits correlation figure: B+ and B- shall be analyzed separately. It is clear in the figure that the slopes are different between B+ and B- for some traits
We add this information to the figure.

Reviewer #2:
The authors would like to thank Reviewer #2 for his suggestions and comments. We carefully read all the points, and we did the necessary modifications. Furthermore, a detailed point-by-point response to all the comments follows below.

Reviewer #2: This paper investigated the response of a maize germplasm panel to PGPB inoculations. The authors studied eleven traits with and without PGPB inoculation and found 30 regions were significant for controlling the symbiosis between PGPB and tropical maize. The authors also conducted subnetwork analysis to identify genes related to negative regulation of the immune system and nitric oxide related processes.

Several suggestions and questions:
1. Page 1 line 12: Your host? Change your to the
We correct this information.

2. This study was carried out in low N conditions. Will the results be the same under normal N conditions?
Preview studies in the literature have shown that the nitrogen status of the soil can negatively impact the symbiotic relationship between the plant and the PGPB (Kox et al., 2016). Based on this, to evaluate the maximum potential of the interaction between maize and PGPB, we decided to conduct our experiment in low N conditions.

3. Show representative images of root phenotypes with and without PGPB inoculation.
We add this information in the supplementary figure 5.

4. It is hard to see the 18 groups in the bar plot. The groups should be clearly labeled in the bar plot. From the cross-validation analysis, it seems 20 has the lowest cross validation error, not 18 in the supplementary figure.
We agree that the 20 groups had the lowest cross validation error. Even though we decided to use the model considering 18 groups to have a more parsimonious model, the increase in the error when we considered 19 groups might indicate model overfitting. In addition, our work aims not to study the population structure, and that is why we omitted the information about the label in the barplot.

5. The color scheme should be changed in the QQplots. It is hard to differentiate the traits. What does the color bar mean for the Manhattan plots?
We remake the figures and add in the supplementary figure 9-11.

6. Page 7 line 23: should be shoot dry mass not dry shoot mass. Page 8 line 5: should be root average diameter (RAD)
We correct this information.

7. Add a coefficient after NF in eq. 1.
We correct this information in the text.

	8. How to explain 0 r2 but still significant for the two SNPs for RAD in table 2? The 0 r2 was due to the rounding when calculating the variance explained. We correct this information in the text. 9. In table 2, the name for the fourth column should be -log10(p-value) not P-value. We correct this information. 10. The hypothesis of this study is maize lines may respond differently to PGPB inoculation. Do a test of the interaction between PGPB treatment and genotypes by combing the two treatments (B+ and B-) together. Is the interaction significant? Add a figure to show the interaction. For example, some genotypes respond to PGPB inoculation while others don't. We performed interaction tests and added this information to the manuscript. The interaction figure shows interactions between B+ and B- treatment, although it wasn't enough to make the LRT test significant. Although, when performing GWAS analysis and genomic prediction models for the Delta treatment, we found important genomic regions controlling the response to the PGPB. REFERENCES Kox, Martine A. R., Claudia Lüke, Christian Fritz, Eva van den Elzen, Theo van Alen, Huub J. M. Op den Camp, Leon P. M. Lamers, Mike S. M. Jetten, and Katharina F. Ettwig. 2016. "Effects of Nitrogen Fertilization on Diazotrophic Activity of Microorganisms Associated with Sphagnum Magellanicum." Plant and Soil 406 (1): 83–100.

On the genetic architecture in a public tropical maize panel of the symbiosis between corn and plant growth-promoting bacteria aiming to improve plant resilience

Rafael Massahiro Yassue[1*], Humberto Fanelli Carvalho[1], Raysa Gevartosky[1], Felipe Sabadin[1], Pedro Henrique Souza[1], Maria Leticia Bonatelli[1], João Lúcio Azevedo[1], Maria Carolina Quecine[1], Roberto Fritsche-Neto[1]

[1]Department of Genetics, Luiz de Queiroz College of Agriculture, University of São Paulo, Piracicaba, São Paulo, Brazil

[*]Corresponding author (e-mail): **rafael.yassue@usp.br**.

RMY: rafael.yassue@usp.br
HFC: humberto.fanelli@gmail.com
RG: raysagevartosky@usp.br
FS: felipe.sabadin@usp.br
PHS: souzaph@usp.br
MLB: mlbonatelli@gmail.com
JLA: jlazevedo@usp.br
MCQ: mquecine@usp.br
RFN: roberto.neto@usp.br

ABSTRACT

Exploring the symbiosis between plants and plant-growth-promoting bacteria (PGPB) is a new challenge for sustainable agriculture. Even though many works have reported the beneficial effects of PGPB in increasing plant resilience for several stresses, its potential is not yet widely explored. One of the many reasons is the differential symbiosis performance depending on the host genotype. This opens doors to plant breeding programs to explore the genetic variability and develop new cultivars with higher response to PGPB interaction and, therefore, have higher resilience to stress. Hence, we aimed to study the genetic architecture of the symbiosis between PGPB and tropical maize germplasm, using a public association panel and its impact on plant resilience. Our findings reveal that the synthetic PGPB population can modulate and impact root architecture traits, improve resilience to nitrogen stress, and 37 regions were significant for controlling the symbiosis between PGPB and tropical maize. We found two overlapping SNPs in the GWAS analysis indicating strong candidates for further investigations. Furthermore, genomic prediction analysis with genomic relationship matrix computed using only significant SNPs obtained from GWAS analysis substantially increased the predictive ability for several traits endorsing the importance of these genomic regions for the response of PGPB. Finally, the public tropical panel reveals a significant genetic variability to the symbiosis with the PGPB and can be a source of alleles to improve plant resilience.

KEYWORDS

Shovelomics; root architecture; GWAS; symbiosis interaction; genomic prediction

DECLARATIONS

Funding and acknowledgment

This study was financed in part by São Paulo Research Foundation (FAPESP, Process: 19/04697-2; 17/24327-0), Coordenação de Aperfeiçoamento de Pessoal de Nível Superior - Brasil (CAPES) - Finance Code 001, and Conselho Nacional de Desenvolvimento Científico e Tecnológico (CNPq).

Conflict of interest

The authors declare no conflict of interest.

Availability of data and material

Genomic data: https://data.mendeley.com/datasets/5gvznd2b3n

Code availability

Code for image processing: https://github.com/RafaelYassue/Root-phenotyping

Ethics approval

Not applicable because this article does not contain any studies with human or animal subjects.

Consent to participate

Not applicable because this article does not contain any studies with human or animal subjects.

Consent for publication

All authors have approved the manuscript and agreed with submission to the Molecular Breeding journal.

INTRODUCTION

Due to the growing need for food (Ray et al. 2013) and environmental pressure (Qi et al. 2018), new approaches that increase production in a sustainable way are required (Gaffney et al. 2019). Tropical agriculture will have to rise to meet the food demand in tropical developing nations (Laurance et al. 2014). Also, studies estimate that it will be necessary to increase the use of fertilizers, with emphasis on N, P_20_5, and K_2O (Pradhan et al. 2015). Furthermore, multidisciplinary research that aims to increase production, sustainability, and plant resilience is justified.

The use of plant growth-promoting bacteria (PGPB) have been a promising field of interest due to the ability to increase production (Martins et al. 2018) and the resilience of the host caused by direct and indirect mechanisms. The most commum mechanism is related to biofertilization, which consists of nutrient uptake and hormones production as well as the ones related to improvement of plant defense (reviewed by (Santoyo et al. 2016; Vejan et al. 2016)). Many studies have proved the benefits of PGPB reducing the plant abiotic stresses caused by salinity (Rojas-Tapias et al. 2012), heavy metals (Gamalero et al. 2009), and drought (Sandhya et al. 2010). However, the use of PGPB as inoculants in agriculture is still incipient.

One of the main challenges of an inoculant with PGPB is the reproducibility of its results in the field (Bashan et al. 2014). Studies have shown that PGPB is influenced by several factors, such as soil type (Egamberdiyeva 2007), nitrogen fertilization (Rodríguez-Blanco et al. 2015), microbe-microbe interaction (Gaiero et al. 2013), and plant-PGPB interactions (Wintermans et al. 2016). In this sense, during the development of a new PGPB inoculant, both environment and genetic factors must be considered (Lemanceau et al. 2017).

In recent years, the genotyping cost has decreased substantially, and its benefits have become consolidated. Currently, one of the gaps for greater gains using genotyping is the poor ability to phenotyping. High-throughput phenotyping (HTP) is a suitable

alternative to increasing phenotyping power (Araus and Cairns 2014). One of the benefits of HTP is measuring secondary traits with direct or indirect effects on primary characteristics (Qiao et al. 2019). For roots, shovelomic analysis has been used to study the root system architecture traits and their impact on the final phenotype (Trachsel et al. 2011).

Evaluation of root architecture is an important tool responsible for the nutrients and water uptaking, which has been the focus of plant breeding for many years (York et al. 2015). In maize, root traits have been identified as key phenotypes to overcome stress in specific environments (Mi et al. 2010; Lynch 2013; Adebayo et al. 2020). Also, in PGPB studies, the root and its architecture play a significant role in the direct interaction with the soil microbiome (Compant et al. 2010). Studies have also revealed that PGPB can modulate root architecture (Gutiérrez-Luna et al. 2010), and the host genotype can influence this response (Wintermans et al. 2016).

Modern plant breeding may have caused a bottleneck in genetic diversity for the symbiosis with PGPB due to the lower response in modern varieties (Valente et al. 2020). In maize, landraces reveal the ability to fix 29%-82% of the plant nitrogen through interaction with PGPB (Van Deynze et al. 2018). Additive and dominance effects have been reported (Vidotti et al. 2019b; Wagner et al. 2020), providing insights into the importance of the host genotype in the impact of PGPB response. GWAS studies have been employed to discover candidate genes to the response of PGPB in *Arabidopsis* (Wintermans et al. 2016; Proietti et al. 2018; Cotta et al. 2020) and maize (Vidotti et al. 2019a).

Based on the genetic variability for the response of PGPB inoculation in many crops, the response of maize to the symbiosis of PGPB may be improved with the support of plant breeding (Kroll et al. 2017; Wei and Jousset 2017) and contribute to more sustainable food production through the increase of yield, sustainability, and plant resilience. Therefore, we aimed to study the symbiosis's genetic architecture between the tropical maize germplasm and a synthetic population of plant growth-promoting bacteria. Also, we present a pipeline for shovelomics evaluation and analysis. Hence, this information

may contribute to plant breeding programs, focusing on new strategies to produce more resilient crops.

MATERIALS AND METHODS

Public tropical maize panel

Our tropical maize germplasm panel contains 360 inbred lines used to analyze the symbiosis's genetic architecture between maize and PGPB. Among them, 183 inbred lines are from ESALQ-USP (Luiz de Queiroz College of Agriculture-University of Sao Paulo) and 173 from IAPAR (Instituto de Desenvolvimento Rural do Paraná). The genomic and phenotypic information about this panel is available on the Mendeley platform (https://data.mendeley.com/datasets/5gvznd2b3n).

Bacterial strain and inoculum

The PGPB *Bacillus thuringiensis* RZ2MS9 and *Delftia* sp. RZ4MS18 were isolated from *Paullinia cupana* (Batista et al. 2018, Batista et al. 2021), *Pantoea agglomerans* 33.1 was isolated from *Eucalyptus grandis* (Quecine et al. 2012), and *Azospirillum brasilense* Ab-v5 is a commercial inoculant (Hungria et al. 2010). They were selected based on previous studies that have reported them as potential inoculants (Batista et al. 2018, Quecine et al. 2012, Hungria et al. 2010) to compose the synthetic population. *In vivo* trials revealed that these PGPB did not have antagonistic effects among each other and, when co-inoculated, promoted growth in maize (unpublished data).

The synthetic population inoculum was prepared by growing each bacterium individually in Luria-Bertani (LB) medium at 28°C with 150 rpm agitation for 24h. The concentration of each bacterium was measured in a spectrophotometer. The synthetic population was composed of each bacteria's adjusted culture medium containing approximatelly 10^8 colony-forming unit/mL. The treatment without PGPB consisted of preparing the inoculum with liquid LB only. Each plot containing three seeds was individually inoculated with 1 ml of the respective treatments, agitated, and sown afterward.

151

152 **Greenhouse experiment**

153 The experiments were carried out under greenhouse conditions at “Luiz de Queiroz”
154 College of Agriculture (ESALQ/USP), Brazil (22˚42'39 "S; 47˚38'09 "W, altitude 540 m). The
155 360 inbred lines were evaluated in two experiments: with (B+) and without (B-) PGPB
156 inoculation. Each experiment was conducted in an augmented blocks design with two replicates
157 across time, each one consisting of six blocks with 60 inbred lines and three common checks.
158 Each replicate of B+ and B- experiments were installed together in a greenhouse. The
159 treatments B+ and B- were physically separated due to the ability of the PGPB to migrate from
160 one to another (Chi et al. 2005; Ji et al. 2010). Furthermore, we calculated the difference
161 between the treatments B+ and B- to compound the Delta. Lastly, we performed analyzes
162 considering the values from B+ and B- individually and the Delta value as a response to the
163 inoculation.

164 In order to evaluate the resilience to N stress and identify genomic regions responsible
165 for the symbiosis between PGPB and maize, we tested the genotypes with and without
166 inoculation with PGPB (B+ and B-, respectively) in low nitrogen conditions similar to (Vidotti et
167 al. 2019a). The low nitrogen condition consisted of no external nitrogen input, and all the
168 nitrogen available to the plants was due to the natural soil organic matter or fixed from PGPB.

169 The maize plants were grown in 3-L plastic pots containing soil. Chemical and
170 physical soil analysis is available in supplementary table 1. The planting fertilization was done
171 according to soil nutrient content and crop demands provided by Soil-app (Matias et al. 2021).
172 It consisted of potassium chloride, simple superphosphate, and limestone soil conditioner inputs
173 added and mixed into the soil. Each plot was sown with three seeds, and after germination, the
174 seedlings were thinning to only one. During the experiments, temperature, radiation, and
175 humidity were monitored and are available in the supplemental figure 1. Twice a week, 200 ml
176 of a complementary fertilizer without nitrogen and adapted from (Hoagland and Snyder 1933)
177 were applied in each plot. Irrigation and other cultural practices were carried out according to
178 the needs of the crop.

Evaluations began when most of the plants were in the V6 growth stage (six expanded leaves). Plant height (PH, cm) was measured from the soil to the last expanded leaf's collar, and the number of expanded leaves was counted (NL). Afterward, the plants were cropped at the soil base, and the stem diameter was measured using a digital caliper (SD, mm). Finally, the harvested shoot (leaves and stem) was dried in a forced draft oven at 60°C for 72h to obtain shoot dry mass (SDM, g).

The roots were carefully washed with water, and each root was stored in plastic pots with a 25% ethanol solution for preservation. Root images were taken to calculate Root Angle (RA, degree, °) and Convex hull area (CHA, cm^2) using a Nikon CoolPix S8100 camera attached to a platform with a fixed height and position. For RA, the images were cropped in order to consider the first 10 centimeters representing the topsoil. These images were processed using a Python script that is available on GitHub (https://github.com/RafaelYassue/Root-phenotyping). Then, new root images were acquired by an Epson LA2400 scanner and processed using the WinRHIZO (Reagent Instruments Inc., Quebec, Canada) to obtain lateral and axial root volume (LRV, ARV, cm^3, respectively), root length (RL, cm), and root average diameter (RAD, mm). Representative images of root phenotypes are available on Supplementary figure 5. The roots were dried out to determine the root dry mass (RDM, g). Furthermore, the ratio of shoot/root (RSR, g g^{-1}) was obtained by dividing the SDM by the RDM.

Phenotypic analysis

To test the interaction between genotype and treatment (B+ and B-) we used the followed full model:

$$\mathbf{y} = \mathbf{X}_1\mathbf{t} + \mathbf{X}_2\mathbf{NL} + \mathbf{Z}_1\mathbf{r} + \mathbf{Z}_2\mathbf{b} + \mathbf{Z}_3\mathbf{g} + \mathbf{Z}_4\mathbf{gt} + \varepsilon \quad \text{Eq. 1}$$

where **y** refers to the phenotypic observation vector, $\mathbf{X}_1$ and $\mathbf{X}_2$ are the incidence matrix for the fixed effect, $\mathbf{Z}_1$, $\mathbf{Z}_2$,$\mathbf{Z}_3$, and $\mathbf{Z}_4$ are the incidence matrices for the random effects. **t** is the fixed effects of treatment (B+ and B-); **r** is random effects of replicates, where $\mathbf{r} \sim N(\mathbf{0}, \mathbf{I}\sigma^2_r)$; **b** is random effects of the block within replicates, where $\mathbf{b} \sim N(\mathbf{0}, \mathbf{I}\sigma^2_b)$; **g** is the vector of

205 random effects of genotype values, where **g** ~ N (**0**, **I**σ^2_g); **gt** is the vector of random effects
206 of the interaction between genotype and treatment, where **gt** ~ N (**0**, **I**σ^2_{gt}); and ε is the
207 random residual effects, where ε ~ N (**0**, **I**σ^2_e). The random effects were tested using the
208 LRT test and the fixed effects using the Wald test. In order to correct the germination and
209 seed vigor differences, the number of leaves (**NL**) was used as a covariable. Spatial
210 analysis and unstructured residual effects were tested, and a good fit of the model was not
211 reached. When we considered the Delta, we used the same above model without the
212 treatment effect, and **y** stands the difference between B+ and B- for each genotype for each
213 trial.

214 After, we obtained the mean-entry heritabilities for each combination of trait and
215 treatment using the reduced model for each treatment (B+,B-, and Delta):

$$\mathbf{y} = \mathbf{X}_1\mathbf{NL} + \mathbf{Z}_1\mathbf{g} + \mathbf{Z}_2\mathbf{r} + \mathbf{Z}_3\mathbf{b} + \varepsilon \quad \text{Eq. 2}$$

216 The heritabilities were calculated at the entry-mean level with the variance
217 components from Eq. 1 and Eq. 2. using the following equations:

$$h^2 = \frac{\sigma_g^2}{\sigma_g^2 + \frac{\sigma_{gt}^2}{r}\frac{\sigma_e^2}{rt}} \quad \text{Eq. 3}$$

218

$$h^2 = \frac{\sigma_g^2}{\sigma_g^2 + \frac{\sigma_e^2}{r}} \quad \text{Eq. 4}$$

219 In which h^2 refers to the mean-entry heritability, σ_g^2, σ_{gt}^2, and σ_e^2 are the variance
220 components due to genotype, the interaction between genotype x treatment, and residual
221 effects, respectively, and r and t is the number of replicates (r = 2) and treatment (t = 2),
222 respectively. The analysis was performed using ASReml-R 4.0 (Butler et al. 2017).

223 We performed a principal component analysis and Pearson correlation between
224 all traits to understand the correlation between traits and their association with the
225 treatments (B+ and B-). The interaction plot was performed using the R package Raincloud

plots (Allen et al. 2021). To simplify a three-way interaction for genotype x treatment x traits, we used reduced model considering genotype effects as a standardized mean of each treatment (B+, B-, Delta) for each trait. After, we performed a Genotype by trait biplot (GT) analysis using the R package metan (Olivoto and Lúcio 2020).

Genotypic data

All 360 tropical inbred lines were genotyped using a genotyping-by-sequencing (GBS) method following the two enzymes (*Pst*I and *Mse*I) protocol (Sim et al. 2012; Poland et al. 2012). The DNA of tropical maize lines was extracted from young and healthy leaves using the CTAB protocol (Doyle and Doyle 1987). Individual genomic DNA samples were digested by restriction enzymes, and samples were included in a sequencing plate. The sequencing was performed on the Illumina NextSeq 500 platform (Illumina Inc., San Diego, CA, United States). Sequence data were aligned against the B73 (B73-RefGen_v4) maize reference genome and the SNP calling was performed using the software TASSEL 5.0 (Bradbury et al. 2007) under default parameters values. The SNP dataset was filtered, and markers with call rate < 90%, non-biallelic, minor allele frequency (MAF) lower than 5%, and heterozygous loci on at least one individual were removed from the dataset, and remaining missing data were imputed by Beagle 5.0 algorithm (Browning et al. 2018). Markers with pairwise linkage disequilibrium (LD) higher than $r^2 > 0.99$ were removed using the SNPRelate package (Zheng et al. 2012). Finally, a total of 13,826 SNPs were considered for the genomic analyses. The coverage and depth of the genotyping-by-sequencing data are shown in the supplementary figure 6.

Population structure and LD decay

The principal components analysis (PCA) regarding the population structure was calculated based on the additive genomic relationship matrix (VanRaden 2008). To identify the most likely number of groups (K) in our panel, we estimated the optimal K-value based on the inferred number of groups producing the lowest cross-validation error using the software ADMIXTURE (Alexander and Lange 2011). We ran the software assuming 2–50 subpopulations using default parameters. We estimated the LD (r^2) between all SNP within

a distance lower than 1 Mbp in the same chromosome, and r^2 values were plotted against base-pair distance to obtain the LD decay by chromosome. To draw a trend line for detecting the LD decay, we used a mean LD in every 100 bases sliding window, where the cutoff r^2 was 0.20.

GWAS analyses

The GWAS analyses were carried out for each combination of trait and inoculation (B+ and B-) and the difference between B+ and B- (Delta) using the FarmCPU R package (Liu et al. 2016). We tested models containing 0 to 6 principal components to correct the population structure effect, and the best model fit was based on QQplot. The Manhattan and QQ plots were obtained using the CMplot R package (Yin et al. 2020). We used the *FarmCPU.P.Threshold* function with 100 permutations to obtain a *p* threshold for each trait. The significant SNPs were annotated using a windows range upstream and downstream, based on LD decay of respective chromosomes (Supplementary figure 8). To obtain the genes on that window, we used the MaizeMine V1.3. (Shamimuzzaman et al. 2020).

Genomic prediction

Genomic predictions (GP) analysis were conducted for each combination of trait x treatment (B+, B-, and Delta). Due to the non-significant effects of the interaction, we did not consider interaction models for the GP analysis. For GP, we used the following three models:

$$\hat{g} = 1u + Za + \varepsilon \qquad \text{GBLUP}$$

$$\hat{g} = 1u + Za + SNPs + \varepsilon \qquad \text{GBLUP\_MAS}$$

$$\hat{g} = 1u + Za + \varepsilon \qquad \text{GMS\_GBLUP}$$

where $\hat{\mathbf{g}}$ is the vector of the adjusted mean for genotype for each treatment (B+, B-, and Delta) from Eq. 2, considering genotype as a fixed effect. **Z** is the incidence matrix of random effects of genotypes, and **a** is the vector of additive effects, where $\mathbf{a} \sim N(0, \mathbf{G}\,\sigma^2_a)$. ε is the vector of random residuals with $\varepsilon \sim N(0, \mathbf{I}\,\sigma^2_\varepsilon)$. **G** is the additive genomic relationship matrix (VanRaden 2008).

For the GBLUP_MAS model, SNPs are the fixed effects of the significant SNPs obtained from the GWAS analysis for each treatment (B+ and B-), except for Delta that the matrix was composed of all significant SNPs from B+, B-, and Delta GWAS analysis. For the model GMS_GBLUP (GWAS Marker Selection GBLUP), genomic additive matrix (**G**) was obtained using only the significant SNPs from the GWAS analysis for each treatment (B+ and B-), except for Delta that we used all significant SNPs. A similar approach for marker selection based on GWAS for genomic prediction is described by Jeong et al. (2020).

In order to evaluate the model performance, we used the CV-α cross-validation with 5 folds and 4 replications (Yassue et al. 2021). The predictive ability of each model was calculated by the Pearson correlation between the predicted and observed values from the validation set.

RESULTS

Exploratory analysis, significance, and heritability

The phenotypic data revealed that the synthetic population of PGPB did promote growth in maize for most traits. For SDM and RDM, the inoculation with PGPB promoted an increase of 12.78% and 20.65%, respectively. Regarding the root's architecture traits, they were also influenced by the inoculation. The plants inoculated with PGPB (B+) tended to have higher values for most root traits, except RA and RSR. Conversely, for RA, RAD, and RSR, the treatment without PGPB (B-) tended to have a higher phenotypic variation. Visual interaction between genotype and treatment can be observed, although its effects were not big enough for significant differences (Figure 1 A). GT biplot analysis revealed the impact of the treatment on the traits. RAD, RDSM, RSR, RA, and SDM showed higher

variance than others traits. On the other hand, PH, CHA, SD, and RL had smaller discrepancies across treatment. RDM and SD were associated with the Delta treatment, while SDM was associated with B+ (Figure 1 B.).

The traits most correlated with SDM were RDM (0.80), ARV (0.71), RL (0.64), LRV (0.56), SD (0.58), PH (0.50), and CHA (0.40) (Supplementary Figure 3). The root traits were also highly correlated (RDM x RL, LRV x RL, LRV x RDM, ARV x RDM). According to PCA analysis (Supplementary Figure 4), we observed that most of the traits were positively associated with bacteria inoculation, except for RA and RSR. Also, it was possible to cluster the genotypes by treatment (B+ and B-).

Significant effects were observed for genotypes and treatment effects for most traits. On the other hand, no interaction effects were observed for the interaction between genotype and treatment (Supplementary Table 2). The heritabilities varied between treatment and among traits. Lower heritabilities were observed for the Delta treatment. PH and SD had the higher heritabilities, meanwhile, root-traits heritabilities tended to be lower (Table 1).

Figure 1. A. Interaction plot considering 360 genotypes with and without inoculation with PGPB (B+, B-, respectively) for eleven traits. **B.** Genotype by traits analysis considering eleven traits and three genotypes (B+, B-, and Delta).

Table 1. Entry mean heritability considering the full model (Eq. 1) and the reduced model for the treatments B+, B-, and Delta (Eq. 2)

Trait	PH	SD	RDM	RL	RAD	LRV	ARV	RA	CHA	SDM	RSR
Full model	0.77	0.67	0.49	0.44	0.43	0.61	0.44	0.34	0.47	0.43	0.51
B+	0.65	0.63	0.35	0.39	0.21	0.54	0.39	0.12	0.32	0.23	0.25
B-	0.63	0.38	0.23	0.31	0.42	0.32	0.34	0.29	0.31	0.20	0.44
Delta	0.08	0.03	0.01	0.13	0.14	0.00	0.14	0.03	0.08	0.00	0.11

Population structure and LD decay

The distribution of r^2 declined as the physical distance increased. The LD decay showed different values across chromosomes (Supplementary Figure 8) and ranged from ~200 kb to ~310 kb, considering the r^2 cutoff of 0.20. The first three principal components from PCA analysis showed that the origins of the genotypes (ESALQ and IAPAR) did not form a prominent group. The ADMIXTURE analysis revealed that the population probably presents 18 groups (Supplementary Figure 7).

GWAS

A total of 13,826 SNPs were used for GWAS analysis for all combinations of traits and treatment (B+, B-, and Delta) (Fig 2). The best good fitness of each model depended on the trait and inoculation. The proportion of the explained variance by significant SNPs ranged from 0.025 to 0.158 (Table 2). There were 30 significant SNPs to the treatment B+, 27 for the treatment B-, and 8 for Delta. Root-traits had a higher number of significant SNPs. No significant SNPs were found for RDM and ARV for B+ treatment, and RDM and RA for B-. Contrastingly, for Delta, we found significant SNPs only for PH, SD, and RDM.

Significant SNPs were found in all chromosomes. The SNP CM000784.4_172073449 was significant for the traits RL, SD, and LRV in the treatment B+. For B- and Delta, no overlapping SNPs were found for different traits. On the other hand, the SNP CM007648.1_169026437 was significant for SD in the treatment B+ and Delta. Based on the LD decay of each chromosome, we identified the genes in linkage disequilibrium with the significant SNPs and found 76 overlapping genes associated

346 simultaneously for B+ and Delta (Fig. 3 A). Meanwhile, no candidate genes were shared
347 between B+ and B-, and B- and Delta. For B+ treatment, 81 overlapping genes were found
348 for three different traits (Fig. 3 B).
349

Figure 2. Circular Manhattan and QQplot for treatment B+ (**A, B**), B- (**C, D**), and Delta (**F**), respectively. Detailed information with Singular Manhattan and QQplot, and SNP information are available on supplementary figures 9 - 11.

354 **Table 2.** Trait, treatment, physical position, MAF, p.values, number of genes, and % of the
355 explained variance for each significant SNP from GWAS analysis

Trait	Treat.	Marker	P.value[a]	MAF	NG.	r^{2b}	Total[c]
PH	B+	CM000780.4_165053545	5.516	0.211	48	0.015	
PH	B+	CM000780.4_241977167	6.809	0.236	74	0.020	
PH	B+	CM000781.4_4105099	5.973	0.314	47	0.012	0.1176
PH	B+	CM000786.4_145397497	5.403	0.183	65	0.011	
PH	B+	CM007649.1_192589545	6.388	0.193	55	0.015	
PH	B+	CM007650.1_99946782	7.789	0.153	8	0.045	
RA	B+	CM007648.1_230920688	10.085	0.207	39	0.043	0.043
CHA	B+	CM000781.4_59021533	7.827	0.132	13	0.033	0.0646
CHA	B+	CM007647.1_27743555	6.608	0.225	36	0.032	
RAD	B+	CM000780.4_23997789	7.442	0.172	25	0.025	0.067
RAD	B+	CM007647.1_215419190	6.934	0.143	31	0.042	
SD	B+	CM000780.4_235759685	7.666	0.286	29	0.027	
SD	B+	CM000782.4_2916367	6.052	0.165	31	0.017	
SD	B+	CM007648.1_38816460	6.755	0.264	45	0.030	0.1584
SD	B+	CM007648.1_169026437	8.497	0.364	21	0.027	
SD	B+	CM007649.1_31624985	7.306	0.081	30	0.031	
SD	B+	CM007650.1_41779668	8.555	0.375	22	0.026	
RL	B+	CM000784.4_172073449	5.652	0.207	81	0.018	0.018
SDM	B+	CM000780.4_181569268	7.142	0.339	57	0.026	
SDM	B+	CM000784.4_172073449	5.325	0.207	81	0.017	0.0866
SDM	B+	CM007647.1_40109546	5.870	0.483	37	0.026	
SDM	B+	CM007648.1_206189255	5.323	0.396	36	0.017	
LRV	B+	CM000780.4_130864198	6.780	0.165	10	0.022	
LRV	B+	CM000784.4_172073449	9.494	0.207	81	0.034	0.0796
LRV	B+	CM007648.1_205666059	6.141	0.196	35	0.024	
RSR	B+	CM000782.4_92896441	9.767	0.083	13	0.033	0.13
RSR	B+	CM000785.4_154128247	7.560	0.385	56	0.020	

RSR	B+	CM007647.1_230383010	5.884	0.064	45	0.036	
RSR	B+	CM007648.1_82524308	6.088	0.288	16	0.019	
RSR	B+	CM007649.1_65858532	6.157	0.276	21	0.019	

[a], $-\log_{10}(p)$
[b], the proportion of phenotypic variance explained by SNP.
[c], Sum of the proportion of phenotypic variance explained by SNPs.

Table 2 (continued)**.** Trait, treatment, physical position, MAF, p.values, number of genes, and % of the explained variance for each significant SNP from GWAS analysis

Trait	Treat.	Marker	P.value[a]	MAF	NG.	r^{2b}	Total[c]
PH	B-	CM000784.4_130925210	5.653	0.186	14	0.018	
PH	B-	CM007647.1_115455586	9.931	0.118	16	0.029	0.0792
PH	B-	CM007647.1_297746433	6.310	0.061	47	0.013	
PH	B-	CM007649.1_57358057	6.887	0.319	34	0.019	
CHA	B-	CM007647.1_29786831	7.069	0.368	33	0.025	0.025
RAD	B-	CM007647.1_299457743	9.082	0.050	43	0.028	
RAD	B-	CM000784.4_173246547	5.632	0.306	70	0.016	
RAD	B-	CM000785.4_148920255	6.834	0.124	41	0.024	0.107
RAD	B-	CM000785.4_149343432	6.122	0.163	54	0.183	
RAD	B-	CM007647.1_190289865	6.001	0.361	43	0.020	
SD	B-	CM000782.4_71684361	8.243	0.228	15	0.042	
SD	B-	CM000785.4_45942495	9.280	0.369	23	0.031	0.1105
SD	B-	CM000785.4_142887012	6.567	0.179	43	0.018	
SD	B-	CM007649.1_13703357	5.947	0.436	32	0.020	
RL	B-	CM000781.4_186664447	9.646	0.188	36	0.036	0.036
SDM	B-	CM000780.4_18077503	6.120	0.344	27	0.021	
SDM	B-	CM007648.1_199939708	7.876	0.283	45	0.027	0.1114
SDM	B-	CM007650.1_12165480	8.585	0.065	20	0.039	
SDM	B-	CM007650.1_159938550	7.202	0.418	37	0.025	
ARV	B-	CM000784.4_176063412	6.230	0.138	54	0.029	
ARV	B-	CM000786.4_143378724	9.735	0.167	48	0.047	0.1043
ARV	B-	CM007649.1_149606256	6.080	0.051	36	0.028	
LRV	B-	CM007647.1_96702974	6.372	0.056	24	0.018	0.036
LRV	B-	CM007648.1_34931191	6.305	0.264	28	0.018	
RSR	B-	CM000780.4_238721378	5.663	0.050	44	0.011	
RSR	B-	CM000784.4_109465968	7.059	0.297	24	0.022	0.051
RSR	B-	CM007647.1_16710073	6.344	0.254	40	0.018	

[a], $-\log_{10}(p)$

[b], the proportion of phenotypic variance explained by SNP.
[c], Sum of the proportion of phenotypic variance explained by SNPs.

Table 2 (continued)**.** Trait, treatment, physical position, MAF, p.values, number of genes, and % of the explained variance for each significant SNP from GWAS analysis

Trait	Treat.	Marker	P.value[a]	MAF	NG.	r^{2b}	Total[c]
PH	Delta	CM000781.4_18267023	5.689	0.293	31	0.039	0.039
SD	Delta	CM000780.4_72636153	7.776	0.302	11	0.03	0.087
SD	Delta	CM000780.4_181664081	5.592	0.286	55	0.015	
SD	Delta	CM007648.1_169026437	5.581	0.363	21	0.017	
SD	Delta	CM007650.1_161417373	6.819	0.307	35	0.025	
RDM	Delta	CM000780.4_243525042	5.643	0.153	84	0.021	0.066
RDM	Delta	CM000781.4_218455951	6.173	0.362	57	0.023	
RDM	Delta	CM007649.1_206185168	5.586	0.052	36	0.022	

[a], $-\log_{10}(p)$
[b], the proportion of phenotypic variance explained by SNP.
[c], Sum of the proportion of phenotypic variance explained by SNPs.

Figure 3. Venn diagrams (**A**) for overlapping genes for the treatments B+, B-, and Delta, and **(B)** for several traits in the treatment B+.

Genomic Prediction

Three genomic prediction models were used in order to evaluate the predictive ability for several traits under different treatments. The first model consisted of using a GBLUP model, the second a GBLUP plus the significant SNPs obtained in the GWAS analysis (GBLUP_MAS) as fixed effects, and the latter using the genomic additive matrix

only the significative SNPs from GWAS (GMS_GBLUP). For the treatment B+, B-, and Delta, the coverage of the SNPs based on the LD decay was 17.43 MBp, 16.90 MBp, and 38.87 MBp, respectively.

The predictive abilities varied across the traits and treatment (B+,B-, and Delta). For all traits, the treatment Delta was the most difficult to predict, meanwhile, B+ and B- had similar performance. A similar performance also was observed between GBLUP and GBLUP_MAS. On the other hand, the use of GMS_GBLUP increased predictive ability for most traits and treatments.

Roots-related traits tended to have lower predictive abilities as well as the Delta treatment. For the treatment Delta and LRV, RA, RAD, RSR, the predictive abilities were near zero, regardless of the genomic prediction model. However, GMS_GBLUP increased predictive abilities for ARV, CHA, PH, RDM, RL, SD, and SDM in the Delta treatment.

Figure 4. Predictive abilities for eleven traits under three treatments (B+, Delta, and B-) and three genomic prediction models (GBLUP, GBLUP_MAS, and GMS_GBLUP).

DISCUSSION

One of the main challenges in the studies with PGPB is to test the potential biostimulant candidates in field conditions due to its high interaction between host genotype and environmental factors (Rouphael et al. 2018). Our study employed greenhouse conditions considering the trade-off between the number of genotypes tested and the real environmental conditions (Rouphael et al. 2018). In addition, early trials may be used to evaluate the final performance of the genotypes (Strigens et al. 2012) and assess the population's genetic variance (Wang et al. 2016). Also, many other studies have considered early plant development as a strategy to select for stress tolerance (Grieder et al. 2014; Obeidat et al. 2018).

Recent studies have shown that the host genotype influences the symbiosis with PGPB, suggesting a host's genetic control (Wintermans et al. 2016; Proietti et al. 2018; Vidotti et al. 2019a). Moreover, the host heterosis plays an important role in shaping bacterial and fungal rhizosphere community composition (Wagner et al. 2020). This is the first study to evaluate the symbiosis between a synthetic population of PGPB and a tropical maize association panel to the best of our knowledge. Our results revealed that the synthetic population of PGPB showed biostimulants effects for most of the genotypes. Also, the PGPB impacted root architecture, and for most traits, influenced the phenotypic variation (Vidotti et al. 2019b). The PGPB benefits in roots have been associated due to the ability of the PGPB to produce plant hormones, such as indole-3-acetic acid (IAA) (Remans et al. 2008), ethylene (Barnawal et al. 2012), abscisic acid (Belimov et al. 2014), gibberellin (Khan et al. 2014), and cytokinins (Liu et al. 2013; Khan et al. 2014).

The strong correlation between root traits and PH, SD, and SDM confirms its importance for absorption and nutrient supply to biomass synthesis. Also, the correlation between root architecture traits revealed a mutual association between them, although GWAS analysis revealed that probably different regions control them. The heritability for root traits was smaller than PH, SD, but they demonstrated potential for selection.

Although we didn't find significant effects for the interaction between genotypes and treatment, we found different SNPs in linkage disequilibrium for the treatment B+ and B- for several traits. The differential association between SNPs and treatments may suggest that other genomic regions are responsible for growth in the presence or absence of PGPB. Furthermore, SNPs associated with the Delta treatment highlight the genetic basis for the response of PGPB. At the same time, it is also possible that these significant SNPs may be functional and not directly related to the bacteria. Further studies should be carried out in order to investigate the genes in these genomics regions and their role in the symbiosis between plant growth-promoting bacteria and maize.

The small heritability for Delta treatment reveals the challenges to evaluate the response to the PGPB. Nevertheless, we found eight significant SNPs associated with three different traits. Overlapping SNPs for the treatments B+ and Delta and others for B+ may indicate the presence of pleiotropic effects or linkage disequilibrium. The magnitude of the LD decay in our population limits the interpretation of our analysis due to the size of the cover of each SNPs, making it difficult to find possible candidate genes for the trait. However, the overlapping genes in the treatments B+ and Delta and from the different traits for B+ can be used as possible candidate genes for further investigation of possible candidate genes for the response to PGPB.

Several studies have been using GWAS and genomic prediction in order to understand the genetic architecture of many traits (Wallace et al. 2016; Galli et al. 2020). Our results revealed that it is possible to increase the predictive ability of several traits when using a subset of SNPs representing important genomic regions, even if the trait heritability is low. The increase in predictive ability, especially in the Delta treatment, when considering only a small part of the genome to compute the GRM, may endorse the importance of these genomic regions for the response to PGPB. Also, these genomic regions can be explored via plant breeding for selection.

Root-traits information seems to be a key to breeding for resilient crops (Lombardi et al. 2021). Besides the difficulty of phenotyping the roots, a large amount of

information generated and how to use this information in the decision-making process is still not fully comprehended. The evaluation of roots is usually laborious due to the need to wash the roots and evaluating them using visual scores (Trachsel et al. 2011) or image analysis (Seethepalli et al. 2021). In our work, we presented a shovelomics pipeline in order to evaluate, analyze, and apply the root traits in the genetic architecture studies and their possible application into plant breeding programs. The predictive ability of RDM, SDM, and most of the traits in the Delta treatment substantially increased when we used the GRM with only the SNPs in disequilibrium with the above and underground traits highlighting the importance of phenotyping these traits (Yonis et al. 2020).

Our results corroborate the hypothesis that multiple genes with small effects are responsible for the response to the PGPB (Cotta et al. 2020). Furthermore, the genetic basis of the response to the PGPB can be used for plant breeding programs to maximize the symbiosis between tropical maize and PGPB and increase plant resilience against biotic and abiotic stress. Also, we suggest that further studies should be conducted in order to validate the SNPs and the genes responsible for the interaction between tropical maize and PGPB.

CONCLUSION

Despite the limitations, our study contributed to understanding the role of the host genotype in the symbiosis with PGPB. In tropical maize, it is controlled by many genes and has a quantitative inheritance. Furthermore, our tropical maize germplasm showed a significant genetic variability to the symbiosis with PGPB, being a good source of alleles for plant breeding programs to develop more resilient genotypes for tropical agriculture.

REFERENCE

Adebayo AR, Kutu FR, Sebetha ET (2020) Data on root system architecture of water efficient maize as affected by different nitrogen fertilizer rates and plant density. Data in Brief 30:105561

Alexander DH, Lange K (2011) Enhancements to the ADMIXTURE algorithm for individual ancestry estimation. BMC Bioinformatics 12:246

Allen M, Poggiali D, Whitaker K, et al (2021) Raincloud plots: a multi-platform tool for robust data visualization. Wellcome Open Res 4:63

Araus JL, Cairns JE (2014) Field high-throughput phenotyping: the new crop breeding frontier. Trends Plant Sci 19:52–61

Barnawal D, Bharti N, Maji D, et al (2012) 1-Aminocyclopropane-1-carboxylic acid (ACC) deaminase-containing rhizobacteria protect Ocimum sanctum plants during waterlogging stress via reduced ethylene generation. Plant Physiol Biochem 58:227–235

Bashan Y, de-Bashan LE, Prabhu SR, Hernandez J-P (2014) Advances in plant growth-promoting bacterial inoculant technology: formulations and practical perspectives (1998–2013). Plant and Soil 378:1–33

Bashan Y, Levanony H (1990) Current status of Azospirillum inoculation technology: Azospirillum as a challenge for agriculture. Canadian Journal of Microbiology 36:591–608

Batista BD, Lacava PT, Ferrari A, et al (2018) Screening of tropically derived, multi-trait plant growth-promoting rhizobacteria and evaluation of corn and soybean colonization ability. Microbiol Res 206:33-42

Batista BD, Dourado MN, Figueredo EF et al (2021) The auxin-producing Bacillus thuringiensis RZ2MS9 promotes the growth and modifies the root architecture of tomato (Solanum lycopersicum cv. Micro-Tom). Arch Microbiol *in press*.

Belimov AA, Dodd IC, Safronova VI, et al (2014) Abscisic acid metabolizing rhizobacteria decrease ABA concentrations in planta and alter plant growth. Plant Physiol Biochem 74:84–91

Bradbury PJ, Zhang Z, Kroon DE, et al (2007) TASSEL: software for association mapping of complex traits in diverse samples. Bioinformatics 23:2633–2635

Browning BL, Zhou Y, Browning SR (2018) A One-Penny Imputed Genome from Next-Generation Reference Panels. Am J Hum Genet 103:338–348

Butler DG, Cullis BR, Gilmour AR, et al (2017) ASReml-R Reference Manual Version 4. VSN International Ltd

Chi F, Shen S-H, Cheng H-P, et al (2005) Ascending migration of endophytic rhizobia, from roots to leaves, inside rice plants and assessment of benefits to rice growth physiology. Appl Environ Microbiol 71:7271–7278

Compant S, Clément C, Sessitsch A (2010) Plant growth-promoting bacteria in the rhizo-

and endosphere of plants: Their role, colonization, mechanisms involved and prospects for utilization. Soil Biology and Biochemistry 42:669–678

Cotta MS, do Amaral FP, Cruz LM, et al (2020) Genome-wide Association Studies Reveal Important Candidate Genes for the Bacillus pumilus TUAT-1-Arabidopsis thaliana Interaction. bioRxiv

Creus CM, Graziano M, Casanovas EM, et al (2005) Nitric oxide is involved in the Azospirillum brasilense-induced lateral root formation in tomato. Planta 221:297–303

Doyle JJ, Doyle JL (1987) A rapid DNA isolation procedure for small quantities of fresh leaf tissue

Egamberdiyeva D (2007) The effect of plant growth promoting bacteria on growth and nutrient uptake of maize in two different soils. Applied Soil Ecology 36:184–189

Gaffney J, Bing J, Byrne PF, et al (2019) Science-based intensive agriculture: Sustainability, food security, and the role of technology. Global Food Security 23:236–244

Gaiero JR, McCall CA, Thompson KA, et al (2013) Inside the root microbiome: bacterial root endophytes and plant growth promotion. Am J Bot 100:1738–1750

Galli G, Alves FC, Morosini JS, Fritsche-Neto R (2020) On the usefulness of parental lines GWAS for predicting low heritability traits in tropical maize hybrids. PLoS One 15:e0228724

Gamalero E, Lingua G, Berta G, Glick BR (2009) Beneficial role of plant growth promoting bacteria and arbuscular mycorrhizal fungi on plant responses to heavy metal stress. Can J Microbiol 55:501–514

Grieder C, Trachsel S, Hund A (2014) Early vertical distribution of roots and its association with drought tolerance in tropical maize. Plant and Soil 377:295–308

Gutiérrez-Luna FM, López-Bucio J, Altamirano-Hernández J, et al (2010) Plant growth-promoting rhizobacteria modulate root-system architecture in Arabidopsis thaliana through volatile organic compound emission. Symbiosis 51:75–83

Hoagland DR, Snyder WC (1933) Nutrition of strawberry plant under controlled conditions : (a) effects of deficiencies of boron and certain other elements : (b) susceptibility to injury from sodium salts. Proceedings of the American Society for Horticultural Science 30:288

Hungria M, Campo RJ, Souza EM, Pedrosa FO (2010) Inoculation with selected strains of *Azospirillum brasilense* and *A. lipoferum* improves yields of maize and wheat in Brazil. Plant Soil 331:413-425

Jeong S, Kim J-Y, Kim N (2020) GMStool: GWAS-based marker selection tool for genomic prediction from genomic data. Sci Rep 10:19653

Ji X, Lu G, Gai Y, et al (2010) Colonization of Morus alba L. by the plant-growth-promoting and antagonistic bacterium Burkholderia cepacia strain Lu10-1. BMC Microbiology 10:243

Kant S, Bi Y-M, Rothstein SJ (2011) Understanding plant response to nitrogen limitation for the improvement of crop nitrogen use efficiency. J Exp Bot 62:1499–1509

564 Khan AL, Waqas M, Kang S-M, et al (2014) Bacterial endophyte Sphingomonas sp. LK11
565 produces gibberellins and IAA and promotes tomato plant growth. J Microbiol
566 52:689–695

567 Khan MIR, Trivellini A, Fatma M, et al (2015) Role of ethylene in responses of plants to
568 nitrogen availability. Front Plant Sci 6:927

569 Kroll S, Agler MT, Kemen E (2017) Genomic dissection of host–microbe and microbe–
570 microbe interactions for advanced plant breeding. Current Opinion in Plant Biology
571 36:71–78

572 Laurance WF, Sayer J, Cassman KG (2014) Agricultural expansion and its impacts on
573 tropical nature. Trends Ecol Evol 29:107–116

574 Lemanceau P, Blouin M, Muller D, Moënne-Loccoz Y (2017) Let the Core Microbiota Be
575 Functional. Trends Plant Sci 22:583–595

576 Liu F, Xing S, Ma H, et al (2013) Cytokinin-producing, plant growth-promoting
577 rhizobacteria that confer resistance to drought stress in Platycladus orientalis
578 container seedlings. Appl Microbiol Biotechnol 97:9155–9164

579 Liu X, Huang M, Fan B, et al (2016) Iterative Usage of Fixed and Random Effect Models
580 for Powerful and Efficient Genome-Wide Association Studies. PLoS Genet
581 12:e1005767

582 Lombardi M, De Gara L, Loreto F (2021) Determinants of Root System Architecture For
583 Future-Ready, Stress-Resilient Crops. Physiol Plant.
584 https://doi.org/10.1111/ppl.13439

585 Lynch JP (2013) Steep, cheap and deep: an ideotype to optimize water and N acquisition
586 by maize root systems. Annals of Botany 112:347–357

587 Martins MR, Jantalia CP, Reis VM, et al (2018) Impact of plant growth-promoting bacteria
588 on grain yield, protein content, and urea-15 N recovery by maize in a Cerrado Oxisol.
589 Plant and Soil 422:239–250

590 Matias FI, Sabadin JFG, Moreira LA, et al (2021) Soil-app: a tool for soil analysis
591 interpretation. Sci Agric 78.: https://doi.org/10.1590/1678-992x-2019-0113

592 Ma W, Li J, Qu B, et al (2014) Auxin biosynthetic gene TAR2 is involved in low nitrogen-
593 mediated reprogramming of root architecture in Arabidopsis. Plant J 78:70–79

594 Mi G, Chen F, Wu Q, et al (2010) Ideotype root architecture for efficient nitrogen
595 acquisition by maize in intensive cropping systems. Sci China Life Sci 53:1369–1373

596 Molina- Favero C, Creus CM, Lanteri ML, et al (2007) Nitric Oxide and Plant Growth
597 Promoting Rhizobacteria: Common Features Influencing Root Growth and
598 Development. Advances in Botanical Research 1–33

599 Obeidat W, Avila L, Earl H, Lukens L (2018) Leaf Spectral Reflectance of Maize
600 Seedlings and Its Relationship to Cold Tolerance. Crop Science 58:2569–2580

601 Olivoto T, Lúcio AD (2020) metan: An R package for multi- environment trial analysis.
602 Methods in Ecology and Evolution 11:783–789

603 Poland JA, Brown PJ, Sorrells ME, Jannink J-L (2012) Development of high-density
604 genetic maps for barley and wheat using a novel two-enzyme genotyping-by-

sequencing approach. PLoS One 7:e32253

Pradhan P, Fischer G, van Velthuizen H, et al (2015) Closing Yield Gaps: How Sustainable Can We Be? PLoS One 10:e0129487

Proietti S, Caarls L, Coolen S, et al (2018) Genome-wide association study reveals novel players in defense hormone crosstalk in Arabidopsis. Plant Cell Environ 41:2342–2356

Qiao S, Fang Y, Wu A, et al (2019) Dissecting root trait variability in maize genotypes using the semi-hydroponic phenotyping platform. Plant and Soil 439:75–90

Qi X, Fu Y, Wang RY, et al (2018) Improving the sustainability of agricultural land use: An integrated framework for the conflict between food security and environmental deterioration. Applied Geography 90:214–223

Quecine MC, Araujo WL, Rossetto PB, et al (2012) Sugarcane Growth Promotion by the Endophytic Bacterium Pantoea agglomerans 33.1. Appl Environ Microb 78:7511-7518

Ray DK, Mueller ND, West PC, Foley JA (2013) Yield Trends Are Insufficient to Double Global Crop Production by 2050. PLoS One 8:e66428

Remans R, Beebe S, Blair M, et al (2008) Physiological and genetic analysis of root responsiveness to auxin-producing plant growth-promoting bacteria in common bean (Phaseolus vulgaris L.). Plant and Soil 302:149–161

Rodríguez-Blanco A, Sicardi M, Frioni L (2015) Plant genotype and nitrogen fertilization effects on abundance and diversity of diazotrophic bacteria associated with maize (Zea mays L.). Biology and Fertility of Soils 51:391–402

Rojas-Tapias D, Moreno-Galván A, Pardo-Díaz S, et al (2012) Effect of inoculation with plant growth-promoting bacteria (PGPB) on amelioration of saline stress in maize (Zea mays). Applied Soil Ecology 61:264–272

Rosier A, Medeiros FHV, Bais HP (2018) Defining plant growth promoting rhizobacteria molecular and biochemical networks in beneficial plant-microbe interactions. Plant and Soil 428:35–55

Rouphael Y, Spíchal L, Panzarová K, et al (2018) High-Throughput Plant Phenotyping for Developing Novel Biostimulants: From Lab to Field or From Field to Lab? Front Plant Sci 9.: https://doi.org/10.3389/fpls.2018.01197

Sandhya V, Ali SZ, Grover M, et al (2010) Effect of plant growth promoting Pseudomonas spp. on compatible solutes, antioxidant status and plant growth of maize under drought stress. Plant Growth Regulation 62:21–30

Santoyo G, Moreno-Hagelsieb G, del Carmen Orozco-Mosqueda M, Glick BR (2016) Plant growth-promoting bacterial endophytes. Microbiological Research 183:92–99

Seethepalli A, Dhakal K, Griffiths M, (2021) et al RhizoVision Explorer: Open-source software for root image analysis and measurement standardization

Shamimuzzaman M, Gardiner JM, Walsh AT, et al (2020) MaizeMine: A Data Mining Warehouse for the Maize Genetics and Genomics Database. Front Plant Sci 11:592730

Sim S-C, Durstewitz G, Plieske J, et al (2012) Development of a Large SNP Genotyping Array and Generation of High-Density Genetic Maps in Tomato. PLoS ONE 7:e40563

Strigens A, Grieder C, Haussmann BIG, Melchinger AE (2012) Genetic Variation among Inbred Lines and Testcrosses of Maize for Early Growth Parameters and Their Relationship to Final Dry Matter Yield. Crop Science 52:1084–1092

Trachsel S, Kaeppler SM, Brown KM, Lynch JP (2011) Shovelomics: high throughput phenotyping of maize (Zea mays L.) root architecture in the field. Plant and Soil 341:75–87

Valente J, Gerin F, Le Gouis J, et al (2020) Ancient wheat varieties have a higher ability to interact with plant growth- promoting rhizobacteria. Plant, Cell & Environment 43:246–260

Van Deynze A, Zamora P, Delaux P-M, et al (2018) Nitrogen fixation in a landrace of maize is supported by a mucilage-associated diazotrophic microbiota. PLOS Biology 16:e2006352

VanRaden PM (2008) Efficient Methods to Compute Genomic Predictions. Journal of Dairy Science 91:4414–4423

Vejan P, Abdullah R, Khadiran T, et al (2016) Role of Plant Growth Promoting Rhizobacteria in Agricultural Sustainability—A Review. Molecules 21:573

Vidotti MS, Lyra DH, Morosini JS, et al (2019a) Additive and heterozygous (dis)advantage GWAS models reveal candidate genes involved in the genotypic variation of maize hybrids to Azospirillum brasilense. PLoS One 14:e0222788

Vidotti MS, Matias FI, Alves FC, et al (2019b) Maize responsiveness to Azospirillum brasilense: Insights into genetic control, heterosis and genomic prediction. PLoS One 14:e0217571

Wagner MR, Roberts JH, Balint- Kurti P, Holland JB (2020) Heterosis of leaf and rhizosphere microbiomes in field- grown maize. New Phytologist 228:1055–1069

Wallace JG, Zhang X, Beyene Y, et al (2016) Genome- wide Association for Plant Height and Flowering Time across 15 Tropical Maize Populations under Managed Drought Stress and Well- Watered Conditions in Sub- Saharan Africa. Crop Science 56:2365–2378

Wang X, Wang H, Liu S, et al (2016) Genetic variation in ZmVPP1 contributes to drought tolerance in maize seedlings. Nat Genet 48:1233–1241

Wei Z, Jousset A (2017) Plant Breeding Goes Microbial. Trends Plant Sci 22:555–558

Wintermans PCA, Bakker PAHM, Pieterse CMJ (2016) Natural genetic variation in Arabidopsis for responsiveness to plant growth-promoting rhizobacteria. Plant Mol Biol 90:623–634

Yassue RM, Sabadin JFG, Galli G, Alves FC (2021) CV-α: designing validations sets to increase the precision and enable multiple comparison tests in genomic prediction. Euphytica 217:106

Yin L, Zhang H, Tang Z, et al (2020) rMVP: A Memory-efficient, Visualization-enhanced, and Parallel-accelerated tool for Genome-Wide Association Study. 2020.08.20.258491

688 Yonis BO, Pino Del Carpio D, Wolfe M, et al (2020) Improving root characterisation for
689 genomic prediction in cassava. Sci Rep 10:8003

690 York LM, Galindo-Castañeda T, Schussler JR, Lynch JP (2015) Evolution of US maize
691 (Zea mays L.) root architectural and anatomical phenes over the past 100 years
692 corresponds to increased tolerance of nitrogen stress. J Exp Bot 66:2347–2358

693 Zheng X, Levine D, Shen J, et al (2012) A high-performance computing toolset for
694 relatedness and principal component analysis of SNP data. Bioinformatics 28:3326–
695 3328

696

697

Figure 1

Click here to access/download;Figure;fig1.png

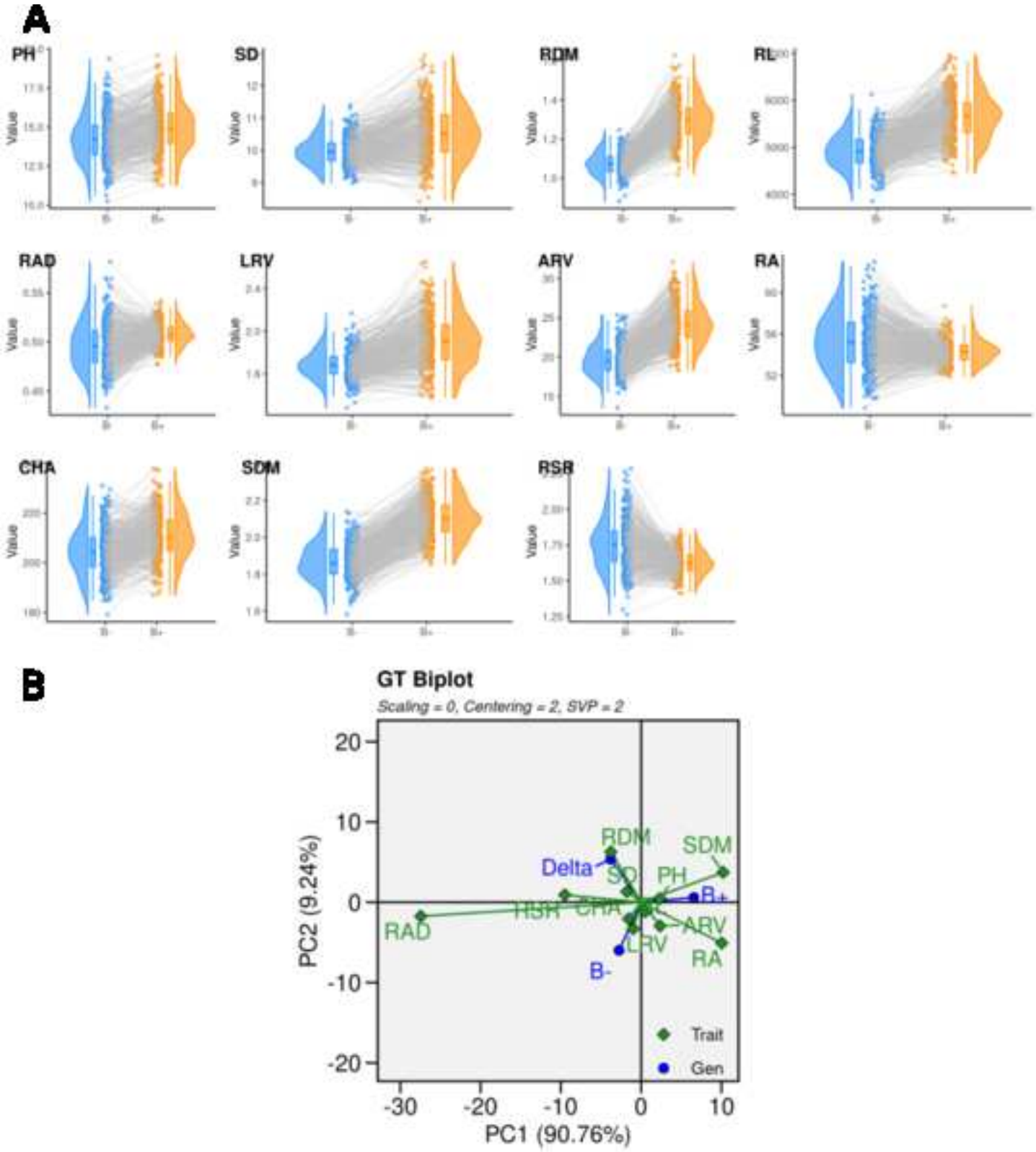

Figure 2

Click here to access/download;Figure;fig2.png

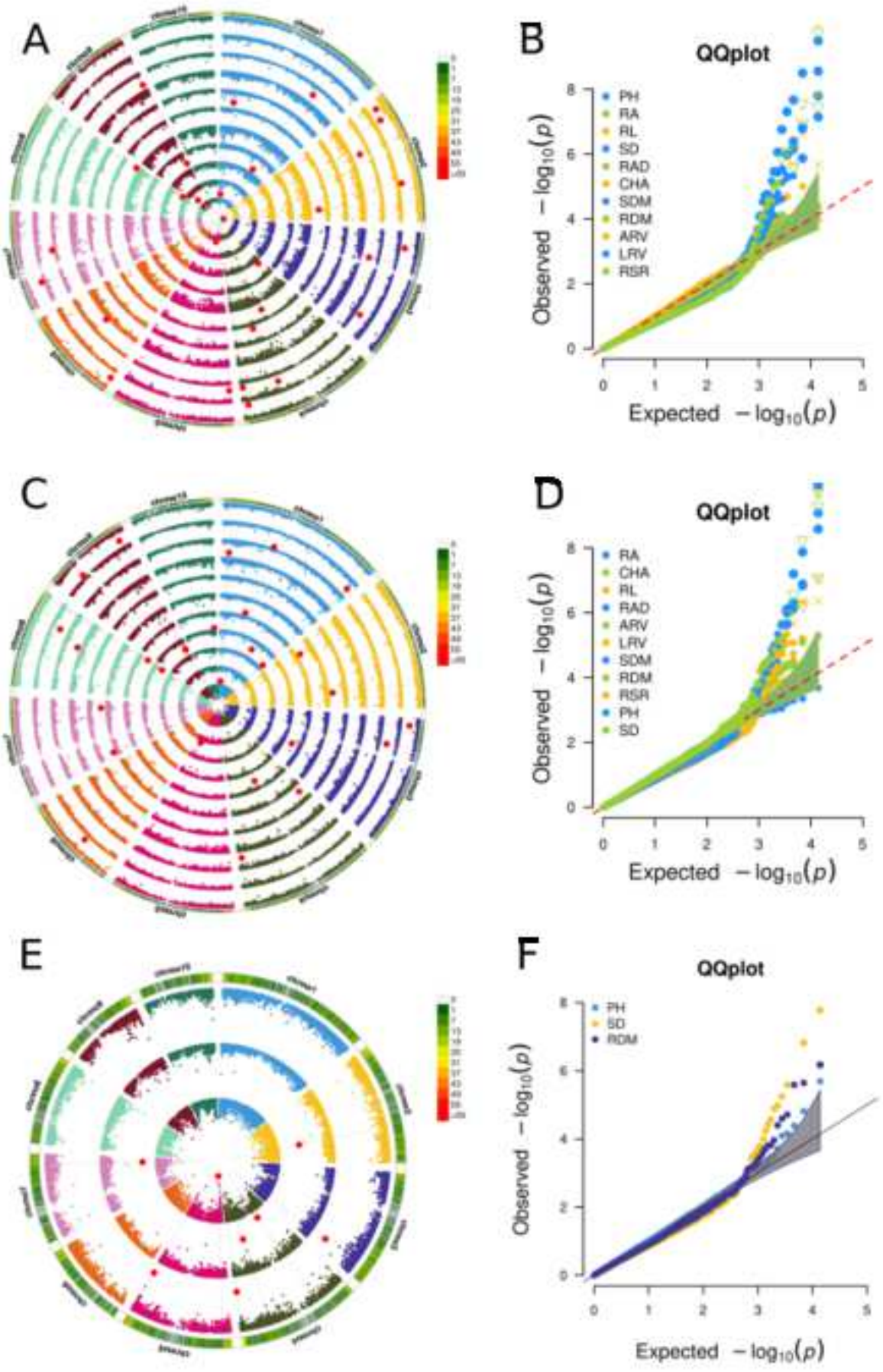

Figure 3

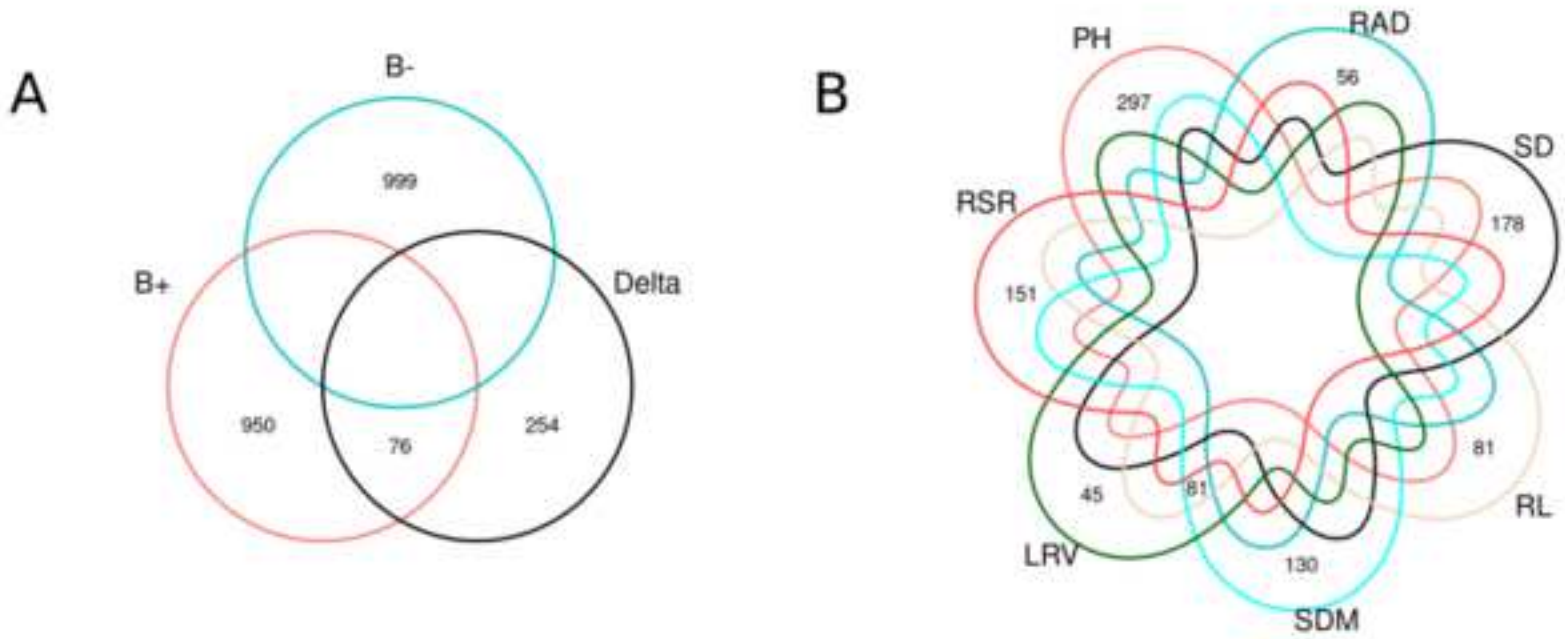

Figure 3

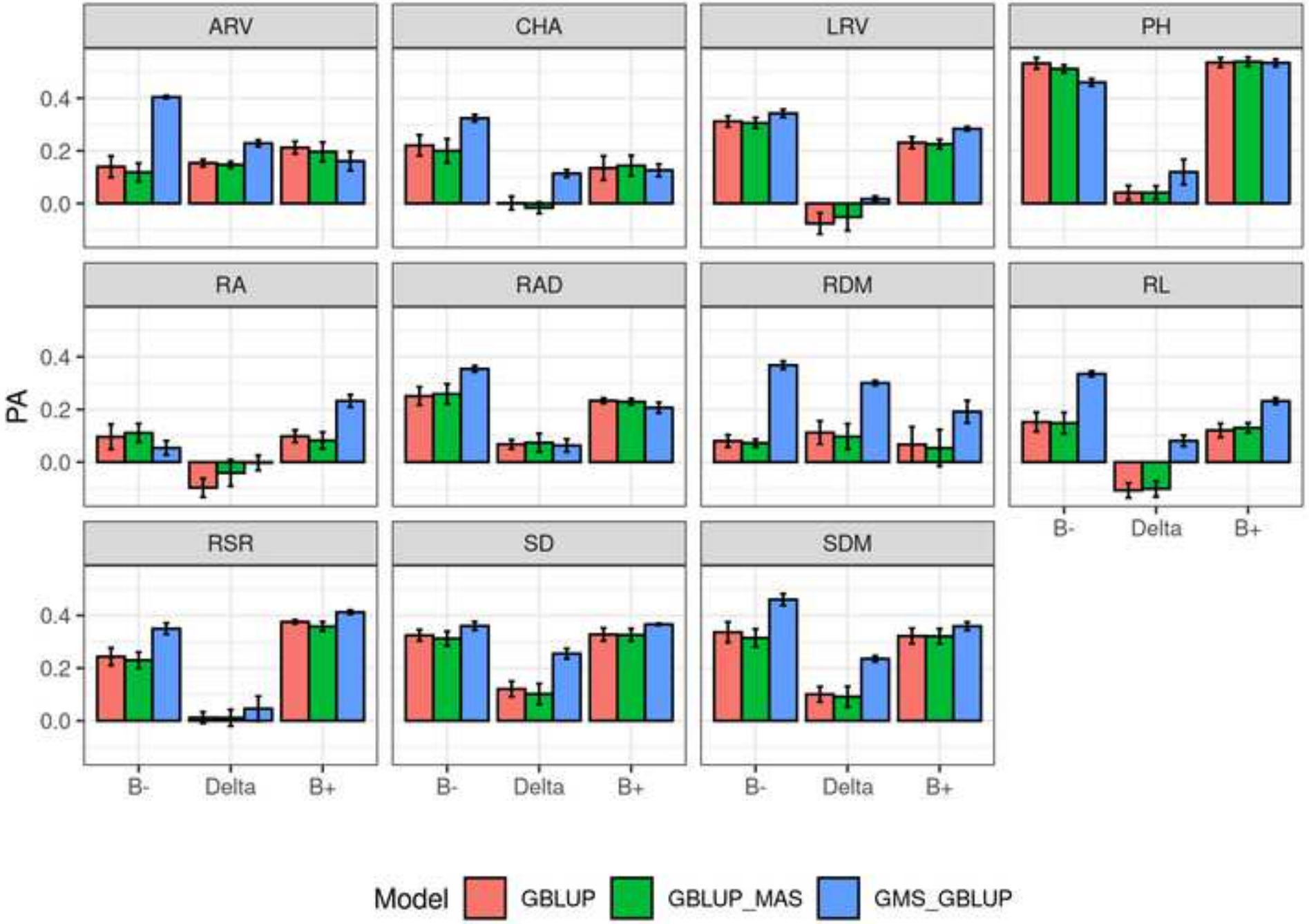

On the genetic architecture in a public tropical maize panel of the symbiosis between corn and plant growth-promoting bacteria aiming to improve plant resilience

Rafael Massahiro Yassue[1*], Humberto Fanelli Carvalho[1], Raysa Gevartosky[1], Felipe Sabadin[1], Pedro Henrique Souza[1], Maria Leticia Bonatelli[1], João Lúcio Azevedo[1], Maria Carolina Quecine[1], Roberto Fritsche-Neto[1]

[1]Department of Genetics, Luiz de Queiroz College of Agriculture, University of São Paulo, Piracicaba, São Paulo, Brazil

[*]Corresponding author (e-mail): **rafael.yassue@usp.br**.

RMY: rafael.yassue@usp.br
HFC: humberto.fanelli@gmail.com
RG: raysagevartosky@usp.br
FS: felipe.sabadin@usp.br
PHS: souzaph@usp.br
MLB: mlbonatelli@gmail.com
JLA: jlazevedo@usp.br
MCQ: mquecine@usp.br
RFN: roberto.neto@usp.br

ABSTRACT

Exploring the symbiosis between plants and plant-growth-promoting bacteria (PGPB) is a new challenge for sustainable agriculture. Even though many works have reported the beneficial effects of PGPB in increasing plant resilience for several stresses, its potential is not yet widely explored. One of the many reasons is the differential symbiosis performance depending on the host genotype. This opens doors to plant breeding programs to explore the genetic variability and develop new cultivars with higher response to PGPB interaction and, therefore, have higher resilience to stress. Hence, we aimed to study the genetic architecture of the symbiosis between PGPB and tropical maize germplasm, using a public association panel and its impact on plant resilience. Our findings reveal that the synthetic PGPB population can modulate and impact root architecture traits, improve resilience to nitrogen stress, and 37 regions were significant for controlling the symbiosis between PGPB and tropical maize. We found two overlapping SNPs in the GWAS analysis indicating strong candidates for further investigations. Furthermore, genomic prediction analysis with genomic relationship matrix computed using only significant SNPs obtained from GWAS analysis substantially increased the predictive ability for several traits endorsing the importance of these genomic regions for the response of PGPB. Finally, the public tropical panel reveals a significant genetic variability to the symbiosis with the PGPB and can be a source of alleles to improve plant resilience.

KEYWORDS

Shovelomics; root architecture; GWAS; symbiosis interaction

DECLARATIONS

Funding and acknowledgment

This study was financed in part by São Paulo Research Foundation (FAPESP, Process: 19/04697-2; 17/24327-0), Coordenação de Aperfeiçoamento de Pessoal de Nível Superior - Brasil (CAPES) - Finance Code 001, and Conselho Nacional de Desenvolvimento Científico e Tecnológico (CNPq).

Conflict of interest

The authors declare no conflict of interest.

Availability of data and material

Genomic data: https://data.mendeley.com/datasets/5gvznd2b3n

Code availability

Code for image processing: https://github.com/RafaelYassue/Root-phenotyping

Ethics approval

Not applicable because this article does not contain any studies with human or animal subjects.

Consent to participate

Not applicable because this article does not contain any studies with human or animal subjects.

Consent for publication

All authors have approved the manuscript and agreed with submission to the Molecular Breeding journal.

INTRODUCTION

Due to the growing need for food (Ray et al. 2013) and environmental pressure (Qi et al. 2018), new approaches that increase production in a sustainable way are required (Gaffney et al. 2019). Tropical agriculture will have to rise to meet the food demand in tropical developing nations (Laurance et al. 2014). Also, studies estimate that it will be necessary to increase the use of fertilizers, with emphasis on N, P_20_5, and K_2O (Pradhan et al. 2015). Furthermore, multidisciplinary research that aims to increase production, sustainability, and plant resilience is justified.

The use of plant growth-promoting bacteria (PGPB) have been a promising field of interest due to the ability to increase production (Martins et al. 2018) and the resilience of the host caused by direct and indirect mechanisms. The most commum mechanism is related to biofertilization, which consists of nutrient uptake and hormones production as well as the ones related to improvement of plant defense (reviewed by (Santoyo et al. 2016; Vejan et al. 2016)). Many studies have proved the benefits of PGPB reducing the plant abiotic stresses caused by salinity (Rojas-Tapias et al. 2012), heavy metals (Gamalero et al. 2009), and drought (Sandhya et al. 2010). However, the use of PGPB as inoculants in agriculture is still incipient.

One of the main challenges of an inoculant with PGPB is the reproducibility of its results in the field (Bashan et al. 2014). Studies have shown that PGPB is influenced by several factors, such as soil type (Egamberdiyeva 2007), nitrogen fertilization (Rodríguez-Blanco et al. 2015), microbe-microbe interaction (Gaiero et al. 2013), and plant-PGPB interactions (Wintermans et al. 2016). In this sense, during the development of a new inoculant, both environment and genetic factors must be considered (Lemanceau et al. 2017).

In recent years, the genotyping cost has decreased substantially, and its benefits have become consolidated. Currently, one of the gaps for greater gains using genotyping is the poor ability to phenotyping. High-throughput phenotyping (HTP) is a suitable

alternative to increasing phenotyping power (Araus and Cairns 2014). One of the benefits of HTP is measuring secondary traits with direct or indirect effects on primary characteristics (Qiao et al. 2019). For roots, shovelomic analysis has been used to study the root system architecture traits and their impact on the final phenotype (Trachsel et al. 2011).

Evaluation of root architecture is an important tool responsible for the nutrients and water uptaking, which has been the focus of plant breeding for many years (York et al. 2015). In maize, root traits have been identified as key phenotypes to overcome stress in specific environments (Mi et al. 2010; Lynch 2013; Adebayo et al. 2020). Also, in PGPB studies, the root and its architecture play a significant role in the direct interaction with the soil microbiome (Compant et al. 2010). Studies have also revealed that PGPB can modulate root architecture (Gutiérrez-Luna et al. 2010), and the host genotype can influence this response (Wintermans et al. 2016).

Modern plant breeding may have caused a bottleneck in genetic diversity for the symbiosis with PGPB due to the lower response in modern varieties (Valente et al. 2020). In maize, landraces reveal the ability to fix 29%-82% of the plant nitrogen through interaction with PGPB (Van Deynze et al. 2018). Additive and dominance effects have been reported (Vidotti et al. 2019b; Wagner et al. 2020), providing insights into the importance of the host genotype in the impact of PGPB response. GWAS studies have been employed to discover candidate genes to the response of PGPB in *Arabidopsis* (Wintermans et al. 2016; Proietti et al. 2018; Cotta et al. 2020) and maize (Vidotti et al. 2019a).

Based on the genetic variability for the response of PGPB inoculation in many crops, the response of maize to the symbiosis of PGPB may be improved with the support of plant breeding (Kroll et al. 2017; Wei and Jousset 2017) and contribute to more sustainable food production through the increase of yield, sustainability, and plant resilience. Therefore, we aimed to study the symbiosis's genetic architecture between the tropical maize germplasm and a synthetic population of plant growth-promoting bacteria. Also, we present a pipeline for shovelomics evaluation and analysis. Hence, this information

may contribute to plant breeding programs, focusing on new strategies to produce more resilient crops.

MATERIALS AND METHODS

Public tropical maize panel

Our tropical maize germplasm panel contains 360 inbred lines used to analyze the symbiosis's genetic architecture between maize and PGPB. Among them, 183 inbred lines are from ESALQ-USP (Luiz de Queiroz College of Agriculture-University of Sao Paulo) and 173 from IAPAR (Instituto de Desenvolvimento Rural do Paraná). The genomic and phenotypic information about this panel is available on the Mendeley platform (https://data.mendeley.com/datasets/5gvznd2b3n).

Bacterial strain and inoculum

The PGPB *Bacillus thuringiensis* RZ2MS9 and *Delftia* sp. RZ4MS18 were isolated from *Paullinia cupana* (Batista et al. 2018, Batista et al. 2021), *Pantoea agglomerans* 33.1 was isolated from *Eucalyptus grandis* (Quecine et al. 2012), and *Azospirillum brasilense* Ab-v5 is a commercial inoculant (Hungria et al. 2010). They were selected based on previous studies that have reported them as potential inoculants (Batista et al. 2018, Quecine et al. 2012, Hungria et al. 2010) to compose the synthetic population. *In vivo* trials revealed that these PGPB did not have antagonistic effects among each other and, when co-inoculated, promoted growth in maize (unpublished data).

The synthetic population inoculum was prepared by growing each bacterium individually in Luria-Bertani (LB) medium at 28°C with 150 rpm agitation for 24h. The concentration of each bacterium was measured in a spectrophotometer. The synthetic population was composed of each bacteria's adjusted culture medium containing approximatelly 10^8 colony-forming unit/mL. The treatment without PGPB consisted of preparing the inoculum with liquid LB only. Each plot containing three seeds was individually inoculated with 1 ml of the respective treatments, agitated, and sown afterward.

Greenhouse experiment

The experiments were carried out under greenhouse conditions at Luiz de Queiroz College of Agriculture (ESALQ/USP), Brazil (22˚42'39 "S; 47˚38'09 "W, altitude 540 m). The 360 inbred lines were evaluated in two experiments: with (B+) and without (B-) PGPB inoculation. Each experiment was conducted in an augmented blocks design with two replicates across time, each one consisting of six blocks with 60 inbred lines and three common checks. Each replicate of B+ and B- experiments were installed together in a greenhouse. The treatments B+ and B- were physically separated due to the ability of the PGPB to migrate from one to another (Chi et al. 2005; Ji et al. 2010). Furthermore, we calculated the difference between the treatments B+ and B- to compound the Delta. Lastly, we performed analyzes considering the values from B+ and B- individually and the Delta value as a response to the inoculation.

In order to evaluate the resilience to N stress and identify genomic regions responsible for the symbiosis between PGPB and maize, we tested the genotypes with and without inoculation with PGPB (B+ and B-, respectively) in low nitrogen conditions similar to (Vidotti et al. 2019a). The low nitrogen condition consisted of no external nitrogen input, and all the nitrogen available to the plants was due to the natural soil organic matter or fixed from PGPB.

The maize plants were grown in 3-L plastic pots containing soil. Chemical and physical soil analysis is available in supplementary table 1. The planting fertilization was done according to soil nutrient content and crop demands provided by Soil-app (Matias et al. 2021). It consisted of potassium chloride, simple superphosphate, and limestone soil conditioner inputs added and mixed into the soil. Each plot was sown with three seeds, and after germination, the seedlings were thinning to only one. During the experiments, temperature, radiation, and humidity were monitored and are available in the supplemental figure 1. Twice a week, 200 ml of a complementary fertilizer without nitrogen and adapted from (Hoagland and Snyder 1933) were applied in each plot. Irrigation and other cultural practices were carried out according to the needs of the crop.

Evaluations began when most of the plants were in the V6 growth stage (six expanded leaves). Plant height (PH, cm) was measured from the soil to the last expanded leaf's collar, and the number of expanded leaves was counted (NL). Afterward, the plants were cropped at the soil base, and the stem diameter was measured using a digital caliper (SD, mm). Finally, the harvested shoot (leaves and stem) was dried in a forced draft oven at 60°C for 72h to obtain dry shoot mass (SDM, g).

The roots were carefully washed with water, and each root was stored in plastic pots with a 25% ethanol solution for preservation. Root images were taken to calculate Root Angle (RA, degree, °) and Convex hull area (CHA, cm^2) using a Nikon CoolPix S8100 camera attached to a platform with a fixed height and position. For RA, the images were cropped in order to consider the first 10 centimeters representing the topsoil. These images were processed using a Python script that is available on GitHub (https://github.com/RafaelYassue/Root-phenotyping). Then, new root images were acquired by an Epson LA2400 scanner and processed using the WinRHIZO (Reagent Instruments Inc., Quebec, Canada) to obtain lateral and axial root volume (LRV, ARV, cm^3, respectively), root length (RL, cm), and average root diameter (RAD, mm). Representative images of root phenotypes are available on Supplementary figure 5. The roots were dried out to determine the root dry mass (RDM, g). The roots were dried out to determine the root dry mass (RDM, g). Furthermore, the ratio of shoot/root (RSR, g g^{-1}) was obtained by dividing the SDM by the RDM.

Phenotypic analysis

To test the interaction between genotype and treatment (B+ and B-) we used the followed full model:

$$\mathbf{y} = \mathbf{X}_1\mathbf{t} + \mathbf{X}_2\mathbf{NL} + \mathbf{Z}_1\mathbf{r} + \mathbf{Z}_2\mathbf{b} + \mathbf{Z}_3\mathbf{g} + \mathbf{Z}_4\mathbf{gt} + \varepsilon \quad \text{Eq. 1}$$

where $\mathbf{y}$ refers to the phenotypic observation vector, $\mathbf{X}_1$ and $\mathbf{X}_2$ are the incidence matrix for the fixed effect, $\mathbf{Z}_1$, $\mathbf{Z}_2$,$\mathbf{Z}_3$, and $\mathbf{Z}_4$ are the incidence matrices for the random effects. $\mathbf{t}$ is the fixed effects of treatment (B+ and B-); $\mathbf{r}$ is random effects of replicates, where $\mathbf{r} \sim N(\mathbf{0}, \mathbf{I}\sigma^2_r)$;

b is random effects of the block within replicates, where **b** ~ N (**0**, **I**σ^2_b); **g** is the vector of random effects of genotype values, where **g** ~ N (**0**, **I**σ^2_g); **gt** is the vector of random effects of the interaction between genotype and treatment, where **gt** ~ N (**0**, **I**σ^2_{gt}); and ε is the random residual effects, where ε ~ N (**0**, **I**σ^2_e). The random effects were tested using the LRT test and the fixed effects using the Wald test. In order to correct the germination and seed vigor differences, the number of leaves (**NL**) was used as a covariable. Spatial analysis and unstructured residual effects were tested, and a good fit of the model was not reached. When we considered the Delta, we used the same above model without the treatment effect, and **y** stands the difference between B+ and B- for each genotype for each trial.

After, we obtained the mean-entry heritabilities for each combination of trait and treatment using the reduced model for each treatment (B+,B-, and Delta):

$$\mathbf{y} = \mathbf{X}_1\mathbf{NL} + \mathbf{Z}_1\mathbf{g} + \mathbf{Z}_2\mathbf{r} + \mathbf{Z}_3\mathbf{b} + \varepsilon \qquad \text{Eq. 2}$$

The heritabilities were calculated at the entry-mean level with the variance components from Eq. 1 and Eq. 2. using the following equations:

$$h^2 = \frac{\sigma_g^2}{\sigma_g^2 + \frac{\sigma_{gt}^2}{r}\frac{\sigma_e^2}{rt}} \qquad \text{Eq. 3}$$

$$h^2 = \frac{\sigma_g^2}{\sigma_g^2 + \frac{\sigma_e^2}{r}} \qquad \text{Eq. 4}$$

In which h^2 refers to the mean-entry heritability, σ_g^2, σ^2 , and σ_e^2 are the variance components due to genotype, the interaction between genotype x treatment, and residual effects, respectively, and r and t is the number of replicates (r = 2) and treatment (t = 2), respectively. The analysis was performed using ASReml-R 4.0 (Butler et al. 2017).

We performed a principal component analysis and Pearson correlation between all traits to understand the correlation between traits and their association with the

treatments (B+ and B-). The interaction plot was performed using the R package Raincloud plots (Allen et al. 2021). To simplify a three-way interaction for genotype x treatment x traits, we used reduced model considering genotype effects as a standardized mean of each treatment (B+, B-, Delta) for each trait. After, we performed a Genotype by trait biplot (GT) analysis using the R package metan (Olivoto and Lúcio 2020).

Genotypic data

All 360 tropical inbred lines were genotyped using a genotyping-by-sequencing (GBS) method following the two enzymes (*Pst*I and *Mse*I) protocol (Sim et al. 2012; Poland et al. 2012). The DNA of tropical maize lines was extracted from young and healthy leaves using the CTAB protocol (Doyle and Doyle 1987). Individual genomic DNA samples were digested by restriction enzymes, and samples were included in a sequencing plate. The sequencing was performed on the Illumina NextSeq 500 platform (Illumina Inc., San Diego, CA, United States). Sequence data were aligned against the B73 (B73-RefGen_v4) maize reference genome and the SNP calling was performed using the software TASSEL 5.0 (Bradbury et al. 2007) under default parameters values. The SNP dataset was filtered, and markers with call rate < 90%, non-biallelic, minor allele frequency (MAF) lower than 5%, and heterozygous loci on at least one individual were removed from the dataset, and remaining missing data were imputed by Beagle 5.0 algorithm (Browning et al. 2018). Markers with pairwise linkage disequilibrium (LD) higher than $r^2 > 0.99$ were removed using the SNPRelate package (Zheng et al. 2012). Finally, a total of 13,826 SNPs were considered for the genomic analyses. The coverage and depth of the genotyping-by-sequencing data are shown in the supplementary figure 6.

Population structure and LD decay

The principal components analysis (PCA) regarding the population structure was calculated based on the additive genomic relationship matrix (VanRaden 2008). To identify the most likely number of groups (K) in our panel, we estimated the optimal K-value based on the inferred number of groups producing the lowest cross-validation error using the software ADMIXTURE (Alexander and Lange 2011). We ran the software assuming 2–50

subpopulations using default parameters. We estimated the LD (r^2) between all SNP within a distance lower than 1 Mbp in the same chromosome, and r^2 values were plotted against base-pair distance to obtain the LD decay by chromosome. To draw a trend line for detecting the LD decay, we used a mean LD in every 100 bases sliding window, where the cutoff r^2 was 0.20.

GWAS analyses

The GWAS analysis were carried out for each combination of trait and inoculation (B+ and B-) and the difference between B+ and B- (Delta) using the FarmCPU R package (Liu et al. 2016). We tested models containing 0 to 6 principal components to correct the population structure effect, and the best model fit was based on QQplot. The Manhattan and QQ plots were obtained using the CMplot R package (Yin et al. 2020). We used the *FarmCPU.P.Threshold* function with 100 permutations to obtain a *p* threshold for each trait. The significant SNPs were annotated using a windows range upstream and downstream, based on LD decay of respective chromosomes (Supplementary figure 8). To obtain the genes on that window, we used the MaizeMine V1.3. (Shamimuzzaman et al. 2020).

Genomic prediction

Genomic predictions (GP) analysis were conducted for each combination of trait x treatment (B+, B-, and Delta). Due to the non-significant effects of the interaction, we did not consider interaction models for the GP analysis. For GP, we used the following three models:

$$\hat{g} = 1\square + Za + \varepsilon \qquad \text{GBLUP}$$

$$\hat{g} = 1\square + Za + SNPs + \varepsilon \qquad \text{GBLUP\_MAS}$$

$$\hat{g} = 1\square + Za + \varepsilon \qquad \text{GMS\_GBLUP}$$

where $\hat{\mathbf{g}}$ is the vector of the adjusted mean for genotype for each treatment (B+, B-, and Delta) from Eq. 2, considering genotype as a fixed effect. **Z** is the incidence matrix of random effects of genotypes, and **a** is the vector of additive effects, where $\mathbf{a} \sim N(0, \mathbf{G}\sigma^2_a)$. ε is the vector of random residuals with □~□(0, □σ^2□). **G** is the additive genomic relationship matrix (VanRaden 2008).

For the GBLUP_MAS model, SNPs are the fixed effects of the significant SNPs obtained from the GWAS analysis for each treatment (B+ and B-), except for Delta that the matrix was composed of all significant SNPs from B+, B-, and Delta GWAS analysis. For the model GMS_GBLUP (GWAS Marker Selection GBLUP), genomic additive matrix (**G**) was obtained using only the significant SNPs from the GWAS analysis for each treatment (B+ and B-), except for Delta that we used all significant SNPs. A similar approach for marker selection based on GWAS for genomic prediction is described by Jeong et al. (2020).

In order to evaluate the model performance, we used the CV-α cross-validation with 5 folds and 4 replications (Yassue et al. 2021). The predictive ability of each model was calculated by the Pearson correlation between the predicted and observed values from the validation set.

RESULTS

Exploratory analysis, significance, and heritability

The phenotypic data revealed that the synthetic population of PGPB did promote growth in maize for most traits. For SDM and RDM, the inoculation with PGPB promoted an increase of 12.78% and 20.65%, respectively. Regarding the root's architecture traits, they were also influenced by the inoculation. The plants inoculated with PGPB (B+) tended to have higher values for most root traits, except RA and RSR. Conversely, for RA, RAD, and RSR, the treatment without PGPB (B-) tended to have a higher phenotypic variation. Visual interaction between genotype and treatment can be observed, although its effects were not big enough for significant differences (Figure 1 A). GT biplot analysis revealed the impact of the treatment on the traits. RAD, RDSM, RSR, RA, and SDM showed higher

variance than others traits. On the other hand, PH, CHA, SD, and RL had smaller discrepancies across treatment. RDM and SD were associated with the Delta treatment, while SDM was associated with B+ (Figure 1 B.).

The traits most correlated with SDM were RDM (0.80), ARV (0.71), RL (0.64), LRV (0.56), SD (0.58), PH (0.50), and CHA (0.40) (Supplementary Figure 3). The root traits were also highly correlated (RDM x RL, LRV x RL, LRV x RDM, ARV x RDM). According to PCA analysis (Supplementary Figure 4), we observed that most of the traits were positively associated with bacteria inoculation, except for RA and RSR. Also, it was possible to cluster the genotypes by treatment (B+ and B-).

Significant effects were observed for genotypes and treatment effects for most traits. On the other hand, no interaction effects were observed for the interaction between genotype and treatment (Supplementary Table 2). The heritabilities varied between treatment and among traits. Lower heritabilities were observed for the Delta treatment. PH and SD had the higher heritabilities, meanwhile, root-traits heritabilities tended to be lower (Table 1).

Figure 1. A. Interaction plot considering 360 genotypes with and without inoculation with PGPB (B+, B-, respectively) for eleven traits. **B.** Genotype by traits analysis considering eleven traits and three genotypes (B+, B-, and Delta).

Table 1. Entry mean heritability considering the full model (Eq. 1) and the reduced model for the treatments B+, B-, and Delta (Eq. 2)

Trait	PH	SD	RDM	RL	RAD	LRV	ARV	RA	CHA	SDM	RSR
Full model	0.77	0.67	0.49	0.44	0.43	0.61	0.44	0.34	0.47	0.43	0.51
B+	0.65	0.63	0.35	0.39	0.21	0.54	0.39	0.12	0.32	0.23	0.25
B-	0.63	0.38	0.23	0.31	0.42	0.32	0.34	0.29	0.31	0.20	0.44
Delta	0.08	0.03	0.01	0.13	0.14	0.00	0.14	0.03	0.08	0.00	0.11

Population structure and LD decay

The distribution of r^2 declined as the physical distance increased. The LD decay showed different values across chromosomes (Supplementary Figure 8) and ranged from ~200 kb to ~310 kb, considering the r^2 cutoff of 0.20. The first three principal components from PCA analysis showed that the origins of the genotypes (ESALQ and IAPAR) did not form a prominent group. The ADMIXTURE analysis revealed that the population probably presents 18 groups (Supplementary Figure 7).

GWAS ~~and Gene Annotation~~

A total of 13,826 SNPs were used for GWAS analysis for all combinations of traits and treatment (B+, B-, and Delta) (Fig 2). The best good fitness of each model depended on the trait and inoculation. The proportion of the explained variance by significant SNPs ranged from 0.025 to 0.158 (Table 2). There were 30 significant SNPs to the treatment B+, 27 for the treatment B-, and 8 for Delta. Root-traits had a higher number of significant SNPs. No significant SNPs were found for RDM and ARV for B+ treatment, and RDM and RA for B-. Contrastingly, for Delta, we found significant SNPs only for PH, SD, and RDM.

Significant SNPs were found in all chromosomes. The SNP CM000784.4_172073449 was significant for the traits RL, SD, and LRV in the treatment B+. For B- and Delta, no overlapping SNPs were found for different traits. On the other hand, the SNP CM007648.1_169026437 was significant for SD in the treatment B+ and Delta. Based on the LD decay of each chromosome, we identified the genes in linkage disequilibrium with the significant SNPs and found 76 overlapping genes associated simultaneously for B+ and Delta (Fig. 3 A). Meanwhile, no candidate genes were shared

between B+ and B-, and B- and Delta. For B+ treatment, 81 overlapping genes were found for three different traits (Fig. 3 B).

We annotated all the genes in the interval based on the LD decay of each chromosome with the significant SNPs. For the treatment with PGPB, we found 1,188 genes and 1,014 genes for the treatment without PGPB in the intervals. We used gene ontology terms and observed a differential co-association between genes with inoculation B+ and B- (Fig 4). For cellular components (Fig 4 A.), differential associations were observed for the ribosome terms, cytosol, endoplasmic reticulum, vacuole, and membrane. Concerning the biological process (Fig 4 B.), a differential association was observed in terms of ribosome biogenesis, generation of precursor metabolites and energy, membrane organization, cytoskeleton organization, homeostatic process, cellular amino acid metabolic process, lipid metabolic process, cellular protein modification process, biosynthetic process, transport, mitotic cell cycle, and complex ribonucleoprotein assembly. For molecular function (Fig 4 C.), differential associations were observed for phosphatase activity, GTPase and DNA-binding transcription factor activity, structural constituent of ribosome, mRNA binding, lipid binding, kinase activity, DNA binding, and ATPase activity.

Using significant genes for each trait and treatment, we performed association analysis with subnetworks enriched for relevant GOBP annotations (gene ontology related to the biological processes) (Fig 5). For B+, two subnetworks were significant for relevant GOBP terms. The genes Zm00001d013067 (GRMZM2G003002) and Zm00001d013066 (GRMZM2G121221) were significative for the subnetwork that negatively regulates the immune system, and Zm00001d032557 (GRMZM2G135866) and Zm00001d032550 (GRMZM2G131591) for nitrogen related process. On the other hand, subnetworks related to B-, the genes Zm00001d012377 (GRMZM2G169341), AC234519.1_FG003, and Zm00001d012375 (GRMZM2G470249) were associated with the response to nitrate (Fig 5A), Zm00001d010322 (GRMZM5G847045) and Zm00001d010322 (GRMZM2G040131) with metabolic process (Fig 6B), and Zm00001d021686 (GRMZM2G076987),

~~Zm00001d021688 (GRMZM2G374309), and Zm00001d021682 (GRMZM2G309380) with nutrient and hormonal response (Fig 6C).~~

Figure 2. Circular Manhattan and QQplot for treatment B+ (**A, B**), B- (**C, D**), and Delta (**F**), respectively. Detailed information with Singular Manhattan and QQplot, and SNP information are available on supplementary figures 9 - 11.

Table 2. Trait, treatment, physical position, MAF, p.values, number of genes, and % of the explained variance for each SNP

Trait	Treat.	Marker	P.value[a]	MAF	NG.	r^{2b}	Total[c]
PH	B+	CM000780.4_165053545	5.516	0.211	48	0.015	
PH	B+	CM000780.4_241977167	6.809	0.236	74	0.020	
PH	B+	CM000781.4_4105099	5.973	0.314	47	0.012	0.1176
PH	B+	CM000786.4_145397497	5.403	0.183	65	0.011	
PH	B+	CM007649.1_192589545	6.388	0.193	55	0.015	
PH	B+	CM007650.1_99946782	7.789	0.153	8	0.045	
RA	B+	CM007648.1_230920688	10.085	0.207	39	0.043	0.043
CHA	B+	CM000781.4_59021533	7.827	0.132	13	0.033	0.0646
CHA	B+	CM007647.1_27743555	6.608	0.225	36	0.032	
RAD	B+	CM000780.4_23997789	7.442	0.172	25	0.025	0.067
RAD	B+	CM007647.1_215419190	6.934	0.143	31	0.042	
SD	B+	CM000780.4_235759685	7.666	0.286	29	0.027	
SD	B+	CM000782.4_2916367	6.052	0.165	31	0.017	
SD	B+	CM007648.1_38816460	6.755	0.264	45	0.030	0.1584
SD	B+	CM007648.1_169026437	8.497	0.364	21	0.027	
SD	B+	CM007649.1_31624985	7.306	0.081	30	0.031	
SD	B+	CM007650.1_41779668	8.555	0.375	22	0.026	
RL	B+	CM000784.4_172073449	5.652	0.207	81	0.018	0.018
SDM	B+	CM000780.4_181569268	7.142	0.339	57	0.026	
SDM	B+	CM000784.4_172073449	5.325	0.207	81	0.017	0.0866
SDM	B+	CM007647.1_40109546	5.870	0.483	37	0.026	
SDM	B+	CM007648.1_206189255	5.323	0.396	36	0.017	
LRV	B+	CM000780.4_130864198	6.780	0.165	10	0.022	
LRV	B+	CM000784.4_172073449	9.494	0.207	81	0.034	0.0796
LRV	B+	CM007648.1_205666059	6.141	0.196	35	0.024	
RSR	B+	CM000782.4_92896441	9.767	0.083	13	0.033	0.13
RSR	B+	CM000785.4_154128247	7.560	0.385	56	0.020	

RSR	B+	CM007647.1_230383010	5.884	0.064	45	0.036	
RSR	B+	CM007648.1_82524308	6.088	0.288	16	0.019	
RSR	B+	CM007649.1_65858532	6.157	0.276	21	0.019	

[a], $-\log_{10}(p)$
[b], the proportion of phenotypic variance explained by SNP.
[c], Sum of the proportion of phenotypic variance explained by SNPs.

Table 2 (continued)**.** Trait, treatment, physical position, MAF, p.values, number of genes, and % of the explained variance for each SNP

Trait	Treat.	Marker	P.value[a]	MAF	NG.	r^{2b}	Total[c]
PH	B-	CM000784.4_130925210	5.653	0.186	14	0.018	
PH	B-	CM007647.1_115455586	9.931	0.118	16	0.029	0.0792
PH	B-	CM007647.1_297746433	6.310	0.061	47	0.013	
PH	B-	CM007649.1_57358057	6.887	0.319	34	0.019	
CHA	B-	CM007647.1_29786831	7.069	0.368	33	0.025	0.025
RAD	B-	CM007647.1_299457743	9.082	0.050	43	0.028	
RAD	B-	CM000784.4_173246547	5.632	0.306	70	0.016	
RAD	B-	CM000785.4_148920255	6.834	0.124	41	0.024	0.107
RAD	B-	CM000785.4_149343432	6.122	0.163	54	0.183	
RAD	B-	CM007647.1_190289865	6.001	0.361	43	0.020	
SD	B-	CM000782.4_71684361	8.243	0.228	15	0.042	
SD	B-	CM000785.4_45942495	9.280	0.369	23	0.031	0.1105
SD	B-	CM000785.4_142887012	6.567	0.179	43	0.018	
SD	B-	CM007649.1_13703357	5.947	0.436	32	0.020	
RL	B-	CM000781.4_186664447	9.646	0.188	36	0.036	0.036
SDM	B-	CM000780.4_18077503	6.120	0.344	27	0.021	
SDM	B-	CM007648.1_199939708	7.876	0.283	45	0.027	0.1114
SDM	B-	CM007650.1_12165480	8.585	0.065	20	0.039	
SDM	B-	CM007650.1_159938550	7.202	0.418	37	0.025	
ARV	B-	CM000784.4_176063412	6.230	0.138	54	0.029	
ARV	B-	CM000786.4_143378724	9.735	0.167	48	0.047	0.1043
ARV	B-	CM007649.1_149606256	6.080	0.051	36	0.028	
LRV	B-	CM007647.1_96702974	6.372	0.056	24	0.018	0.036
LRV	B-	CM007648.1_34931191	6.305	0.264	28	0.018	
RSR	B-	CM000780.4_238721378	5.663	0.050	44	0.011	
RSR	B-	CM000784.4_109465968	7.059	0.297	24	0.022	0.051
RSR	B-	CM007647.1_16710073	6.344	0.254	40	0.018	

[a], $-\log_{10}(p)$

[b], the proportion of phenotypic variance explained by SNP.
[c], Sum of the proportion of phenotypic variance explained by SNPs.

Table 2 (continued)**.** Trait, treatment, physical position, MAF, p.values, number of genes, and % of the explained variance for each SNP

Trait	Treat.	Marker	P.value[a]	MAF	NG.	r^{2b}	Total[c]
PH	Delta	CM000781.4_18267023	5.689	0.293	31	0.039	0.039
SD	Delta	CM000780.4_72636153	7.776	0.302	11	0.03	0.087
SD	Delta	CM000780.4_181664081	5.592	0.286	55	0.015	
SD	Delta	CM007648.1_169026437	5.581	0.363	21	0.017	
SD	Delta	CM007650.1_161417373	6.819	0.307	35	0.025	
RDM	Delta	CM000780.4_243525042	5.643	0.153	84	0.021	0.066
RDM	Delta	CM000781.4_218455951	6.173	0.362	57	0.023	
RDM	Delta	CM007649.1_206185168	5.586	0.052	36	0.022	

[a], $-\log_{10}(p)$
[b], the proportion of phenotypic variance explained by SNP.
[c], Sum of the proportion of phenotypic variance explained by SNPs.

A B

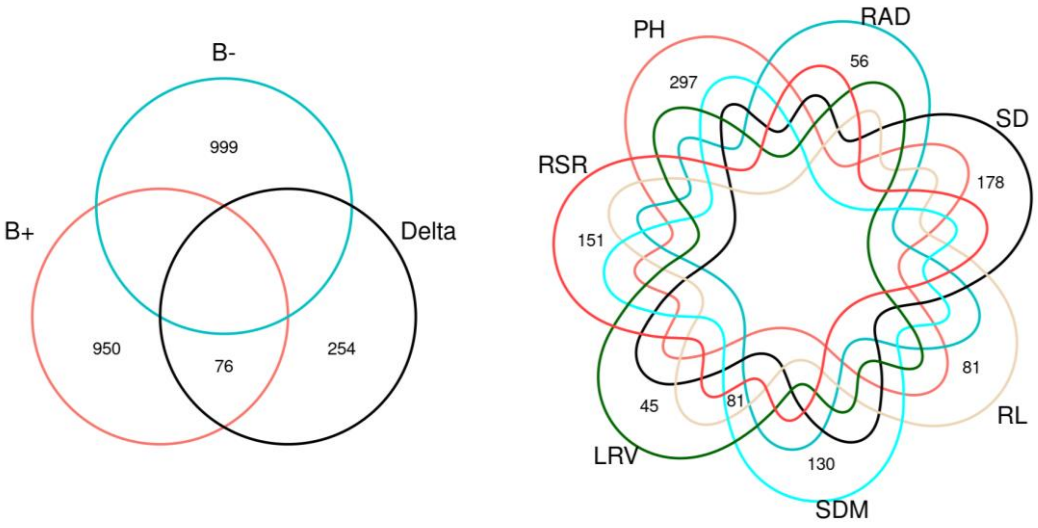

Figure 3. Venn diagrams (**A**) for overlapping genes for the treatments B+, B-, and Delta, and **(B)** for several traits in the treatment B+.

~~**Figure 4.** Most frequent enriched GO terms for candidate genes found by GWAS analysis divided by **A.** cellular component, **B.** biological process, and **C.** molecular function.~~

~~**Figure 5.** Subnetwork enrichment analysis associated with relevant annotation for traits with inoculation. The nodes with bold edges represent the significative candidate genes from GWAS, and the orange nodes are associated with the subnetwork gene ontology. The gene ontology for the networks is **A.** negative regulation of the immune system (PH). **B.** Nitric oxide metabolic process, Negative regulation of nitric-oxide synthase activity, and Reactive nitrogen species metabolic process (RSR).~~

~~**Figure 6.** Subnetwork enrichment analysis associated with relevant annotation for traits with no inoculation. The nodes with bold edges represent the significant candidate genes from GWAS, and the orange nodes are associated with the gene ontology annotation of the subnetwork. The gene ontology for the networks is **A.** response to nitrate (RAD). **B.**~~

~~negative regulation of the metabolic process, regulation of nitrogen compound metabolic process (RSR). **C.** Cellular response to nitrogen levels, response to nutrient, cellular response to abiotic stimulus, salicylic acid metabolic process, response to ethylene, response to nutrient levels, response to nitrate, regulation of hormone levels, and auxin transport (SDM).~~

Genomic Prediction

Three genomic prediction models were used in order to evaluate the predictive ability for several traits under different treatments. The first model consisted of using a GBLUP model, the second a GBLUP plus the significant SNPs obtained in the GWAS analysis (GBLUP_MAS) as fixed effects, and the latter using the genomic additive matrix only the significative SNPs from GWAS (GMS_GBLUP). For the treatment B+, B-, and Delta, the coverage of the SNPs based on the LD decay was 17.43 MBp, 16.90 MBp, and 38.87 MBp, respectively.

The predictive abilities varied across the traits and treatment (B+,B-, and Delta). For all traits, the treatment Delta was the most difficult to predict, meanwhile, B+ and B- had similar performance. A similar performance also was observed between GBLUP and GBLUP_MAS. On the other hand, the use of GMS_GBLUP increased predictive ability for most traits and treatments.

Roots-related traits tended to have lower predictive abilities as well as the Delta treatment. For the treatment Delta and LRV, RA, RAD, RSR, the predictive abilities were near zero, regardless of the genomic prediction model. However, GMS_GBLUP increased predictive abilities for ARV, CHA, PH, RDM, RL, SD, and SDM in the Delta treatment.

Figure 4. Predictive abilities for eleven traits under three treatments (B+, Delta, and B-) and three genomic prediction models (GBLUP, GBLUP_MAS, and GMS_GBLUP).

DISCUSSION

One of the main challenges in the studies with PGPB is to test the potential biostimulant candidates in field conditions due to its high interaction between host genotype and environmental factors (Rouphael et al. 2018). Our study employed greenhouse conditions considering the trade-off between the number of genotypes tested and the real environmental conditions (Rouphael et al. 2018). In addition, early trials may be used to evaluate the final performance of the genotypes (Strigens et al. 2012) and assess the population's genetic variance (Wang et al. 2016). Also, many other studies have considered early plant development as a strategy to select for stress tolerance (Grieder et al. 2014; Obeidat et al. 2018).

Recent studies have shown that the host genotype influences the symbiosis with PGPB, suggesting a host's genetic control (Wintermans et al. 2016; Proietti et al. 2018; Vidotti et al. 2019a). Moreover, the host heterosis plays an important role in shaping bacterial and fungal rhizosphere community composition (Wagner et al. 2020). This is the first study to evaluate the symbiosis between a synthetic population of PGPB and a tropical maize association panel to the best of our knowledge. Our results revealed that the synthetic population of PGPB showed biostimulants effects for most of the genotypes. Also, the PGPB impacted root architecture, and for most traits, influenced the phenotypic variation (Vidotti et al. 2019b). The PGPB benefits in roots have been associated due to the ability of the PGPB to produce plant hormones, such as indole-3-acetic acid (IAA) (Remans et al. 2008), ethylene (Barnawal et al. 2012), abscisic acid (Belimov et al. 2014), gibberellin (Khan et al. 2014), and cytokinins (Liu et al. 2013; Khan et al. 2014).

The strong correlation between root traits and PH, SD, and SDM confirms its importance for absorption and nutrient supply to biomass synthesis. Also, the correlation between root architecture traits revealed a mutual association between them, although GWAS analysis revealed that probably different regions control them. The heritability for root traits was smaller than PH, SD, but they demonstrated potential for selection.

Although we didn't find significant effects for the interaction between genotypes and treatment, we found different SNPs in linkage disequilibrium for the treatment B+ and B- for several traits. The differential association between SNPs and treatments may suggest that other genomic regions are responsible for growth in the presence or absence of PGPB. Furthermore, SNPs associated with the Delta treatment highlight the genetic basis for the response of PGPB. At the same time, it is also possible that these significant SNPs may be functional and not directly related to the bacteria. Further studies should be carried out in order to investigate the genes in these genomics regions and their role in the symbiosis between plant growth-promoting bacteria and maize.

The small heritability for Delta treatment reveals the challenges to evaluate the response to the PGPB. Nevertheless, we found eight significant SNPs associated with three different traits. Overlapping SNPs for the treatments B+ and Delta and others for B+ may indicate the presence of pleiotropic effects or linkage disequilibrium. The magnitude of the LD decay in our population limits the interpretation of our analysis due to the size of the cover of each SNPs, making it difficult to find possible candidate genes for the trait. However, the overlapping genes in the treatments B+ and Delta and from the different traits for B+ can be used as possible candidate genes for further investigation of possible candidate genes for the response of PGPB.

Several studies have been using GWAS and genomic prediction in order to understand the genetic architecture of many traits (Wallace et al. 2016; Galli et al. 2020). Our results revealed that it is possible to increase the predictive ability of several traits when using a subset of SNPs representing important genomic regions, even if the trait heritability is low. The increase in predictive ability, especially in the Delta treatment, when considering only a small part of the genome to compute the GRM, may endorse the importance of these genomic regions for the response to PGPB. Also, these genomic regions can be explored via plant breeding for selection.

Root-traits information seems to be a key to breeding for resilient crops (Lombardi et al. 2021). Besides the difficulty of phenotyping the roots, a large amount of

information generated and how to use this information in the decision-making process is still not fully comprehended. The evaluation of roots is usually laborious due to the need to wash the roots and evaluating them using visual scores (Trachsel et al. 2011) or image analysis (Seethepalli et al. 2021). In our work, we presented a shovelomics pipeline in order to evaluate, analyze, and apply the root traits in the genetic architecture studies and their possible application into plant breeding programs. The predictive ability of RDM, SDM, and most of the traits in the Delta treatment substantially increased when we used the GRM with only the SNPs in disequilibrium with the above and underground traits highlighting the importance of phenotyping these traits (Yonis et al. 2020).

Our results corroborate the hypothesis that multiple genes with small effects are responsible for the response to the PGPB (Cotta et al. 2020). Furthermore, the genetic basis of the response to the PGPB can be used for plant breeding programs to maximize the symbiosis between tropical maize and PGPB and increase plant resilience against biotic and abiotic stress. Also, we suggest that further studies should be conducted in order to validate the SNPs and the genes responsible for the interaction between tropical maize and PGPB.

~~The annotation of significant SNPs revealed that many genes were obtained in both treatments due to the extensive LD decay in our population. However, these differences in the significant SNPs due to the inoculation (B+ and B) reveal different genomic regions associated with growth when the PGPB is inoculated. The annotation showed that they are differentially related to cellular components, biological process, and molecular function based on the significant candidate genes. The candidate gene Zm00001d013070 for the treatment with inoculation was also found significantly (Vidotti et al. 2019a) under N stress, suggesting that this gene may be related to the response to the N.main difficulty is probably related to the quantitative genetic control of the symbiosis with PGPB, which has many traits and pathways controlling it.~~

~~On the other hand, for the treatment without inoculation of PGPB and low availability of nitrogen, different subnetworks were associated with the candidate genes. The association~~

~~with response to nitrate, ethylene, auxin, and cellular response to abiotic stimulus indicates that the genes were associated with nitrogen use efficiency (NUE) (Kant et al. 2011; Ma et al. 2014; Khan et al. 2015). The higher number of subnetworks found in the treatment without inoculation was probably due to the origin of the stress once that nitrogen stress has been studied and more subnetworks are reported. Even though the finding of candidate genes to NUE is essential, this is not the focus of this work. Still, they can be applied to other studies and are available as supplementary materials.~~

~~Multiple significative genes with small effects and subnetworks with different gene ontology corroborate with the hypothesis that the benefits of the PGPB involve numerous mechanisms and the final phenotype is the sum of them (Bashan and Levanony 1990) contributing to the results found in the literature (Cotta et al. 2020).~~

CONCLUSION

Despite the limitations, our study contributed to understanding the role of the host genotype in the symbiosis with PGPB. In tropical maize, it is controlled by many genes and has a quantitative inheritance. Furthermore, our tropical maize germplasm showed a significant genetic variability to the symbiosis with PGPB, being a good source of alleles for plant breeding programs to develop more resilient genotypes for tropical agriculture.

REFERENCE

Adebayo AR, Kutu FR, Sebetha ET (2020) Data on root system architecture of water efficient maize as affected by different nitrogen fertilizer rates and plant density. Data in Brief 30:105561

Alexander DH, Lange K (2011) Enhancements to the ADMIXTURE algorithm for individual ancestry estimation. BMC Bioinformatics 12:246

Allen M, Poggiali D, Whitaker K, et al (2021) Raincloud plots: a multi-platform tool for robust data visualization. Wellcome Open Res 4:63

Araus JL, Cairns JE (2014) Field high-throughput phenotyping: the new crop breeding frontier. Trends Plant Sci 19:52–61

Barnawal D, Bharti N, Maji D, et al (2012) 1-Aminocyclopropane-1-carboxylic acid (ACC) deaminase-containing rhizobacteria protect Ocimum sanctum plants during waterlogging stress via reduced ethylene generation. Plant Physiol Biochem 58:227–235

Bashan Y, de-Bashan LE, Prabhu SR, Hernandez J-P (2014) Advances in plant growth-promoting bacterial inoculant technology: formulations and practical perspectives (1998–2013). Plant and Soil 378:1–33

Bashan Y, Levanony H (1990) Current status of Azospirillum inoculation technology: Azospirillum as a challenge for agriculture. Canadian Journal of Microbiology 36:591–608

Batista BD, Lacava PT, Ferrari A, et al (2018) Screening of tropically derived, multi-trait plant growth-promoting rhizobacteria and evaluation of corn and soybean colonization ability. Microbiol Res 206:33-42

Batista BD, Dourado MN, Figueredo EF et al (2021) The auxin-producing Bacillus thuringiensis RZ2MS9 promotes the growth and modifies the root architecture of tomato (Solanum lycopersicum cv. Micro-Tom). Arch Microbiol *in press*.

Belimov AA, Dodd IC, Safronova VI, et al (2014) Abscisic acid metabolizing rhizobacteria decrease ABA concentrations in planta and alter plant growth. Plant Physiol Biochem 74:84–91

Bradbury PJ, Zhang Z, Kroon DE, et al (2007) TASSEL: software for association mapping of complex traits in diverse samples. Bioinformatics 23:2633–2635

Browning BL, Zhou Y, Browning SR (2018) A One-Penny Imputed Genome from Next-Generation Reference Panels. Am J Hum Genet 103:338–348

Butler DG, Cullis BR, Gilmour AR, et al (2017) ASReml-R Reference Manual Version 4. VSN International Ltd

Chi F, Shen S-H, Cheng H-P, et al (2005) Ascending migration of endophytic rhizobia, from roots to leaves, inside rice plants and assessment of benefits to rice growth physiology. Appl Environ Microbiol 71:7271–7278

Compant S, Clément C, Sessitsch A (2010) Plant growth-promoting bacteria in the rhizo-

and endosphere of plants: Their role, colonization, mechanisms involved and prospects for utilization. Soil Biology and Biochemistry 42:669–678

Cotta MS, do Amaral FP, Cruz LM, et al (2020) Genome-wide Association Studies Reveal Important Candidate Genes for the Bacillus pumilus TUAT-1-Arabidopsis thaliana Interaction. bioRxiv

Creus CM, Graziano M, Casanovas EM, et al (2005) Nitric oxide is involved in the Azospirillum brasilense-induced lateral root formation in tomato. Planta 221:297–303

Doyle JJ, Doyle JL (1987) A rapid DNA isolation procedure for small quantities of fresh leaf tissue

Egamberdiyeva D (2007) The effect of plant growth promoting bacteria on growth and nutrient uptake of maize in two different soils. Applied Soil Ecology 36:184–189

Gaffney J, Bing J, Byrne PF, et al (2019) Science-based intensive agriculture: Sustainability, food security, and the role of technology. Global Food Security 23:236–244

Gaiero JR, McCall CA, Thompson KA, et al (2013) Inside the root microbiome: bacterial root endophytes and plant growth promotion. Am J Bot 100:1738–1750

Galli G, Alves FC, Morosini JS, Fritsche-Neto R (2020) On the usefulness of parental lines GWAS for predicting low heritability traits in tropical maize hybrids. PLoS One 15:e0228724

Gamalero E, Lingua G, Berta G, Glick BR (2009) Beneficial role of plant growth promoting bacteria and arbuscular mycorrhizal fungi on plant responses to heavy metal stress. Can J Microbiol 55:501–514

Grieder C, Trachsel S, Hund A (2014) Early vertical distribution of roots and its association with drought tolerance in tropical maize. Plant and Soil 377:295–308

Gutiérrez-Luna FM, López-Bucio J, Altamirano-Hernández J, et al (2010) Plant growth-promoting rhizobacteria modulate root-system architecture in Arabidopsis thaliana through volatile organic compound emission. Symbiosis 51:75–83

Hoagland DR, Snyder WC (1933) Nutrition of strawberry plant under controlled conditions : (a) effects of deficiencies of boron and certain other elements : (b) susceptibility to injury from sodium salts. Proceedings of the American Society for Horticultural Science 30:288

Hungria M, Campo RJ, Souza EM, Pedrosa FO (2010) Inoculation with selected strains of *Azospirillum brasilense* and *A. lipoferum* improves yields of maize and wheat in Brazil. Plant Soil 331:413-425

Jeong S, Kim J-Y, Kim N (2020) GMStool: GWAS-based marker selection tool for genomic prediction from genomic data. Sci Rep 10:19653

Ji X, Lu G, Gai Y, et al (2010) Colonization of Morus alba L. by the plant-growth-promoting and antagonistic bacterium Burkholderia cepacia strain Lu10-1. BMC Microbiology 10:243

Kant S, Bi Y-M, Rothstein SJ (2011) Understanding plant response to nitrogen limitation for the improvement of crop nitrogen use efficiency. J Exp Bot 62:1499–1509

Khan AL, Waqas M, Kang S-M, et al (2014) Bacterial endophyte Sphingomonas sp. LK11 produces gibberellins and IAA and promotes tomato plant growth. J Microbiol 52:689–695

Khan MIR, Trivellini A, Fatma M, et al (2015) Role of ethylene in responses of plants to nitrogen availability. Front Plant Sci 6:927

Kroll S, Agler MT, Kemen E (2017) Genomic dissection of host–microbe and microbe–microbe interactions for advanced plant breeding. Current Opinion in Plant Biology 36:71–78

Laurance WF, Sayer J, Cassman KG (2014) Agricultural expansion and its impacts on tropical nature. Trends Ecol Evol 29:107–116

Lemanceau P, Blouin M, Muller D, Moënne-Loccoz Y (2017) Let the Core Microbiota Be Functional. Trends Plant Sci 22:583–595

Liu F, Xing S, Ma H, et al (2013) Cytokinin-producing, plant growth-promoting rhizobacteria that confer resistance to drought stress in Platycladus orientalis container seedlings. Appl Microbiol Biotechnol 97:9155–9164

Liu X, Huang M, Fan B, et al (2016) Iterative Usage of Fixed and Random Effect Models for Powerful and Efficient Genome-Wide Association Studies. PLoS Genet 12:e1005767

Lombardi M, De Gara L, Loreto F (2021) Determinants of Root System Architecture For Future-Ready, Stress-Resilient Crops. Physiol Plant. https://doi.org/10.1111/ppl.13439

Lynch JP (2013) Steep, cheap and deep: an ideotype to optimize water and N acquisition by maize root systems. Annals of Botany 112:347–357

Martins MR, Jantalia CP, Reis VM, et al (2018) Impact of plant growth-promoting bacteria on grain yield, protein content, and urea-15 N recovery by maize in a Cerrado Oxisol. Plant and Soil 422:239–250

Matias FI, Sabadin JFG, Moreira LA, et al (2021) Soil-app: a tool for soil analysis interpretation. Sci Agric 78.: https://doi.org/10.1590/1678-992x-2019-0113

Ma W, Li J, Qu B, et al (2014) Auxin biosynthetic gene TAR2 is involved in low nitrogen-mediated reprogramming of root architecture in Arabidopsis. Plant J 78:70–79

Mi G, Chen F, Wu Q, et al (2010) Ideotype root architecture for efficient nitrogen acquisition by maize in intensive cropping systems. Sci China Life Sci 53:1369–1373

Molina- Favero C, Creus CM, Lanteri ML, et al (2007) Nitric Oxide and Plant Growth Promoting Rhizobacteria: Common Features Influencing Root Growth and Development. Advances in Botanical Research 1–33

Obeidat W, Avila L, Earl H, Lukens L (2018) Leaf Spectral Reflectance of Maize Seedlings and Its Relationship to Cold Tolerance. Crop Science 58:2569–2580

Olivoto T, Lúcio AD (2020) metan: An R package for multi- environment trial analysis. Methods in Ecology and Evolution 11:783–789

Poland JA, Brown PJ, Sorrells ME, Jannink J-L (2012) Development of high-density genetic maps for barley and wheat using a novel two-enzyme genotyping-by-

sequencing approach. PLoS One 7:e32253

Pradhan P, Fischer G, van Velthuizen H, et al (2015) Closing Yield Gaps: How Sustainable Can We Be? PLoS One 10:e0129487

Proietti S, Caarls L, Coolen S, et al (2018) Genome-wide association study reveals novel players in defense hormone crosstalk in Arabidopsis. Plant Cell Environ 41:2342–2356

Qiao S, Fang Y, Wu A, et al (2019) Dissecting root trait variability in maize genotypes using the semi-hydroponic phenotyping platform. Plant and Soil 439:75–90

Qi X, Fu Y, Wang RY, et al (2018) Improving the sustainability of agricultural land use: An integrated framework for the conflict between food security and environmental deterioration. Applied Geography 90:214–223

Quecine MC, Araujo WL, Rossetto PB, et al (2012) Sugarcane Growth Promotion by the Endophytic Bacterium Pantoea agglomerans 33.1. Appl Environ Microb 78:7511-7518

Ray DK, Mueller ND, West PC, Foley JA (2013) Yield Trends Are Insufficient to Double Global Crop Production by 2050. PLoS One 8:e66428

Remans R, Beebe S, Blair M, et al (2008) Physiological and genetic analysis of root responsiveness to auxin-producing plant growth-promoting bacteria in common bean (Phaseolus vulgaris L.). Plant and Soil 302:149–161

Rodríguez-Blanco A, Sicardi M, Frioni L (2015) Plant genotype and nitrogen fertilization effects on abundance and diversity of diazotrophic bacteria associated with maize (Zea mays L.). Biology and Fertility of Soils 51:391–402

Rojas-Tapias D, Moreno-Galván A, Pardo-Díaz S, et al (2012) Effect of inoculation with plant growth-promoting bacteria (PGPB) on amelioration of saline stress in maize (Zea mays). Applied Soil Ecology 61:264–272

Rosier A, Medeiros FHV, Bais HP (2018) Defining plant growth promoting rhizobacteria molecular and biochemical networks in beneficial plant-microbe interactions. Plant and Soil 428:35–55

Rouphael Y, Spíchal L, Panzarová K, et al (2018) High-Throughput Plant Phenotyping for Developing Novel Biostimulants: From Lab to Field or From Field to Lab? Front Plant Sci 9.: https://doi.org/10.3389/fpls.2018.01197

Sandhya V, Ali SZ, Grover M, et al (2010) Effect of plant growth promoting Pseudomonas spp. on compatible solutes, antioxidant status and plant growth of maize under drought stress. Plant Growth Regulation 62:21–30

Santoyo G, Moreno-Hagelsieb G, del Carmen Orozco-Mosqueda M, Glick BR (2016) Plant growth-promoting bacterial endophytes. Microbiological Research 183:92–99

Seethepalli A, Dhakal K, Griffiths M, (2021) et al RhizoVision Explorer: Open-source software for root image analysis and measurement standardization

Shamimuzzaman M, Gardiner JM, Walsh AT, et al (2020) MaizeMine: A Data Mining Warehouse for the Maize Genetics and Genomics Database. Front Plant Sci 11:592730

Sim S-C, Durstewitz G, Plieske J, et al (2012) Development of a Large SNP Genotyping Array and Generation of High-Density Genetic Maps in Tomato. PLoS ONE 7:e40563

Strigens A, Grieder C, Haussmann BIG, Melchinger AE (2012) Genetic Variation among Inbred Lines and Testcrosses of Maize for Early Growth Parameters and Their Relationship to Final Dry Matter Yield. Crop Science 52:1084–1092

Trachsel S, Kaeppler SM, Brown KM, Lynch JP (2011) Shovelomics: high throughput phenotyping of maize (Zea mays L.) root architecture in the field. Plant and Soil 341:75–87

Valente J, Gerin F, Le Gouis J, et al (2020) Ancient wheat varieties have a higher ability to interact with plant growth- promoting rhizobacteria. Plant, Cell & Environment 43:246–260

Van Deynze A, Zamora P, Delaux P-M, et al (2018) Nitrogen fixation in a landrace of maize is supported by a mucilage-associated diazotrophic microbiota. PLOS Biology 16:e2006352

VanRaden PM (2008) Efficient Methods to Compute Genomic Predictions. Journal of Dairy Science 91:4414–4423

Vejan P, Abdullah R, Khadiran T, et al (2016) Role of Plant Growth Promoting Rhizobacteria in Agricultural Sustainability—A Review. Molecules 21:573

Vidotti MS, Lyra DH, Morosini JS, et al (2019a) Additive and heterozygous (dis)advantage GWAS models reveal candidate genes involved in the genotypic variation of maize hybrids to Azospirillum brasilense. PLoS One 14:e0222788

Vidotti MS, Matias FI, Alves FC, et al (2019b) Maize responsiveness to Azospirillum brasilense: Insights into genetic control, heterosis and genomic prediction. PLoS One 14:e0217571

Wagner MR, Roberts JH, Balint- Kurti P, Holland JB (2020) Heterosis of leaf and rhizosphere microbiomes in field- grown maize. New Phytologist 228:1055–1069

Wallace JG, Zhang X, Beyene Y, et al (2016) Genome- wide Association for Plant Height and Flowering Time across 15 Tropical Maize Populations under Managed Drought Stress and Well- Watered Conditions in Sub- Saharan Africa. Crop Science 56:2365–2378

Wang X, Wang H, Liu S, et al (2016) Genetic variation in ZmVPP1 contributes to drought tolerance in maize seedlings. Nat Genet 48:1233–1241

Wei Z, Jousset A (2017) Plant Breeding Goes Microbial. Trends Plant Sci 22:555–558

Wintermans PCA, Bakker PAHM, Pieterse CMJ (2016) Natural genetic variation in Arabidopsis for responsiveness to plant growth-promoting rhizobacteria. Plant Mol Biol 90:623–634

Yassue RM, Sabadin JFG, Galli G, Alves FC (2021) CV-α: designing validations sets to increase the precision and enable multiple comparison tests in genomic prediction. Euphytica 217:106

Yin L, Zhang H, Tang Z, et al (2020) rMVP: A Memory-efficient, Visualization-enhanced, and Parallel-accelerated tool for Genome-Wide Association Study. 2020.08.20.258491

Yonis BO, Pino Del Carpio D, Wolfe M, et al (2020) Improving root characterisation for genomic prediction in cassava. Sci Rep 10:8003

York LM, Galindo-Castañeda T, Schussler JR, Lynch JP (2015) Evolution of US maize (Zea mays L.) root architectural and anatomical phenes over the past 100 years corresponds to increased tolerance of nitrogen stress. J Exp Bot 66:2347–2358

Zheng X, Levine D, Shen J, et al (2012) A high-performance computing toolset for relatedness and principal component analysis of SNP data. Bioinformatics 28:3326–3328